

1 **The Aare main overdeepening on the northern margin of the European Alps: Basins, riegels,**
2 **and slot canyons**

3
4 Fritz Schlunegger¹, Edi Kissling², Dimitri Bandou^{1,3}, Guilhem Douillet¹, David Mair¹, Urs Marti⁴,
5 Regina Reber¹, Patrick Schläfli^{1,5}, and Michael Schwenk^{1,6}

6
7 ¹Institute of Geological Sciences, University of Bern, Baltzerstrasse 1+3, 3012 Bern, Switzerland

8 ²Department of Earth Sciences, ETH Zürich, Sonneggstrasse 5, 8092 Zürich, Switzerland

9 ³Department of Environmental Sciences, University of Virginia, 291 McCormick Rd., Charlottesville,
10 VA 22904-4123, USA

11 ⁴Landesgeologie Swisstopo, Seftigenstrasse 264, Postfach, 3084 Wabern, Switzerland

12 ⁵Institute of Plant Sciences and Oeschger Centre for Climate Change Research, Altenbergrain 21,
13 3013 Bern, Switzerland

14 ⁶Bayerisches Landesamt für Umwelt, Umweltdienstleistungen, Hof, 95030 Hof Saale, Germany

15
16 fritz.schlunegger@unibe.ch

17
18 **Abstract**

19 This work summarizes the results of an interdisciplinary project where we aimed to explore the origin
20 of overdeepenings through a combination of a gravimetry survey, drillings and dating. To this end, we
21 focused on the Bern area, Switzerland, situated on the northern margin of the European Alps. This area
22 experienced multiple advances of piedmont glaciers during the Quaternary glaciations, resulting in the
23 carving of the main overdeepening of the Aare River valley (referred to as the Aare main
24 overdeepening). This bedrock depression is tens of km long and up to several hundreds of m to a few
25 km wide. We found that in the Bern area, the Aare main overdeepening is made up of two >200 m-deep
26 troughs that are separated by a c. 5 km-long and up to 150 m-high transverse rocky ridge, interpreted
27 as a riegel. The basins and the riegel are overlain by a >200 m- and a c. 100 m-thick succession of
28 Quaternary sediments, respectively. The bedrock itself is made up of a Late Oligocene to Early Miocene
29 suite of consolidated clastic deposits, which are part of the Molasse foreland basin. In contrast, the
30 Quaternary suite comprises a middle Pleistocene to Holocene succession of unconsolidated glacio-
31 lacustrine gravel, sand and mud. A synthesis of published gravimetry data revealed that the upstream
32 stoss side of the bedrock riegel is c. 50% flatter than the downstream lee side. In addition, information
33 from >100 deep drillings reaching depths >50 m suggests that the bedrock riegel is dissected by an
34 anastomosing network of slot canyons. Apparently, the slot canyons established the hydrological
35 connection between the upstream and downstream basins during their formation. Based on published
36 modelling results, we interpret that the riegels and canyons were formed through incision of subglacial

Deleted: Overdeepening or tunnel valley of the Aare glacier...

Formatted: English (UK)

Deleted: Dimitry

Formatted: English (UK)

Formatted: English (UK)

Field Code Changed

Formatted: English (UK)

Formatted: English (UK)

Formatted: English (UK)

Deleted: or tunnel valleys

Deleted: ,

Deleted: and a synthesis of previously published work

Formatted: English (UK)

Formatted: English (UK)

Formatted: English (UK)

Deleted: In this region,

Deleted: resulted

Formatted: English (UK)

Formatted: English (UK)

Formatted: English (UK)

Deleted: meters

Formatted: English (UK)

Deleted: kilometers

Deleted: this

Formatted: English (UK)

Formatted: English (UK)

Formatted: English (UK)

Deleted: , whereas

Formatted: English (UK)

Formatted: English (UK)

Deleted: We propose that these

Formatted: English (UK)

50 meltwater during a glacier's decay state, when large volumes of meltwater were released. It appears
 51 that such a situation has repeatedly occurred since the Middle Pleistocene Transition approximately 800
 52 ka ago, when large, several hundreds of m-thick and erosive piedmont glaciers began to advance far
 53 into the foreland. This resulted in the deep carving of the inner-Alpine valleys and additionally in the
 54 formation of overdeepenings, riegels and slot canyons, on the plateau situated on the northern margin of
 55 the Alps.

57 1 Introduction

58 Overdeepenings are bedrock depressions below the current fluvial base-level (e.g., Jørgensen and
 59 Sandersen, 2006; Dürst Stucki et al., 2010; 2013; Fischer and Häberli, 2012). The downstream closures
 60 of these basins have adverse slopes that generally dip in the upstream direction (Häberli et al., 2016).
 61 Because bedrock depressions with such characteristics (Figure 1) are commonly found in previously
 62 glaciated areas, their formation has been interpreted as resulting from the erosional work of glaciers
 63 and/or subglacial meltwater (Wright, 1973; Herman and Braun, 2008; Egholm et al., 2009; Kehew et
 64 al., 2012; Patton et al., 2016; Liebl et al., 2023; and many others). Overdeepenings have been reported
 65 for the Quaternary from beneath the Greenland and Antarctic glaciers (Ross et al., 2011; Patton et al.,
 66 2016), but also in the North Sea (Moreau et al., 2012, Lohrberg et al., 2022), North America (Wright,
 67 1973; Lloyd et al., 2023) and northern Europe including Scandinavia (Clark and Walder, 1994;
 68 Piotrowski, 1997; Krohn et al., 2009). Glaciogenic paleovalleys are not only limited to the Quaternary
 69 but were also described for Paleozoic glaciations (e.g. Douillet et al., 2012; Dietrich et al., 2021). In the
 70 European Alps, such erosional troughs occur in Alpine valleys as well as on foreland plateaus on either
 71 side of this mountain belt (Preusser et al., 2010; Dürst Stucki and Schlunegger, 2013; Magrani et al.,
 72 2020). Pollen analysis (Welten, 1982; 1988; Schlüchter, 1989; Schläfli et al., 2021), dating using
 73 optically stimulating luminescence methods (Preusser et al., 2005; Dehnert et al., 2012; Büchi et al.,
 74 2018; Schwenk et al., 2022a) and ¹⁴C ages established on organic matter encountered in the
 75 overdeepening fill (Kellerhals and Häfeli, 1984) showed that these troughs were formed after the Middle
 76 Pleistocene Transition, which occurred c. 800 ka ago (Schlüchter, 2004). Geophysical surveys (e.g.,
 77 Rosselli and Raymond, 2003; Reitner et al., 2010; Stewart and Lonergan, 2011; Stewart et al., 2013;
 78 Perrouy et al., 2015; Burschil et al., 2018; 2019; Ottesen et al., 2020) in combination with drillings
 79 (Jordan, 2010; Dürst Stucki et al., 2010; Büchi et al., 2017; 2018; Gegg et al., 2021; Bandou et al., 2022;
 80 2023; Anselmetti et al., 2022; Schwenk et al., 2022a, b; Gegg and Preusser, 2023; Schaller et al., 2023)
 81 disclosed that such overdeepenings can be several km wide, tens of km long and >200 m deep. The
 82 surveys also showed that overdeepenings are typically composed of individual sub-basins, separated by
 83 bedrock swells or bumps oriented transverse to the flow of a former glacier, hereafter called riegels
 84 (Cook and Swift, 2012), yet the specific details of such a geometry have not yet been elaborated.

- Deleted: Such
- Formatted (... [1])
- Deleted: ,
- Formatted (... [2])
- Deleted: , or tunnel valleys (
- Formatted: English (UK)
- Deleted:),
- Formatted: English (UK)
- Moved (insertion) [1]
- Formatted (... [3])
- Deleted: (Figure 1),
- Formatted: English (UK)
- Deleted: with support by
- Formatted (... [4])
- Deleted: Kron
- Deleted: In addition, numerous Paleozoic successions entailing glaciogenic
- Formatted: English (UK)
- Formatted (... [5])
- Deleted: Such
- Deleted: have particularly been identified in the European Alps (Preusser et al., 2010), where >200 m-deep and several km-long bedrock depressions beneath the modern base-level
- Formatted: English (UK)
- Deleted: the
- Formatted: English (UK)
- Formatted (... [6])
- Deleted: kilometers
- Deleted: and
- Deleted: kilometers
- Formatted: English (UK)
- Formatted: English (UK)
- Formatted (... [7])
- Deleted: they
- Deleted: generally made up
- Formatted: English (UK)
- Formatted (... [8])
- Deleted: ,
- Formatted (... [9])
- Deleted:). Bedrock swells or riegels that separate bedrock depressions
- Deleted: also
- Deleted: reported from modern landscapes. In this cor (... [10])
- Formatted: English (UK)
- Formatted: English (UK)
- Formatted: English (UK)

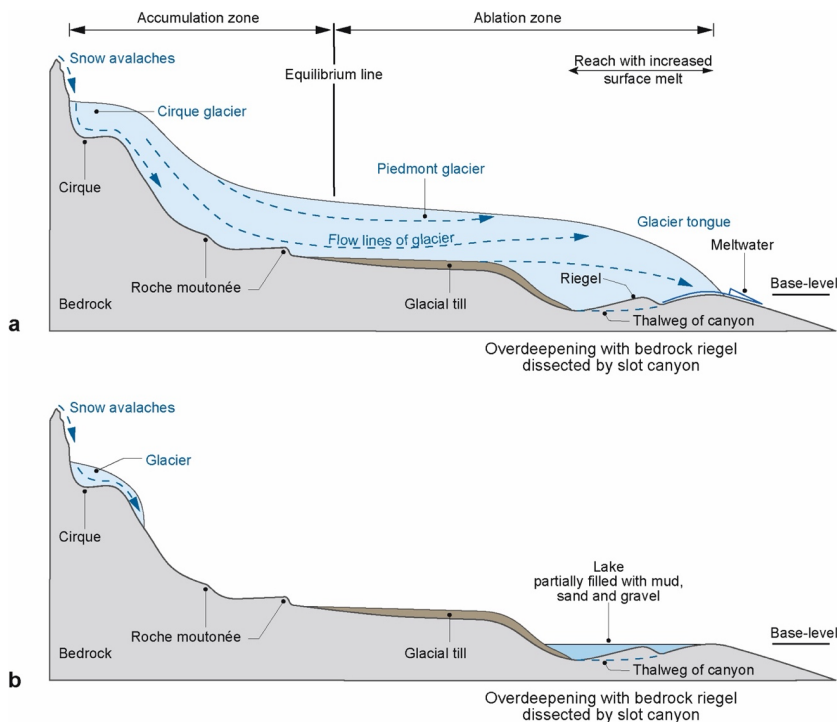


Figure 1

Figure 1: Architecture of a landscape sculpted by piedmont glaciers during glaciations. a) Situation immediately following a full glacial period during which a piedmont glacier, which extended far into the foreland, started to melt. As a result, large volumes of meltwater are produced in the ablation zone close to the glacier's tongue. This meltwater has the potential to contribute to the erosional downwearing of the bedrock, and it can cause the incision of canyons into bedrock riegels, which separate two overdeepened basins. b) During interglacial time periods, the piedmont glaciers disappear, and small ice caps may be preserved in the higher parts of a mountain belt. During this time, the overdeepened basin will be filled by lacustrine sediments and/or will eventually host a lake. Modified after Schlunegger and Garefalakis (2023).

Here, we summarize the results of an interdisciplinary project where we aim to explore the origin of overdeepenings using a combination of data collected through a gravimetry survey (Bandou, 2023a; Bandou et al., 2022, 2023), drillings (Reber and Schlunegger, 2016; Schwenk et al., 2022a, b) and dating (Schläfli et al., 2021; Schwenk et al., 2022a). We focus our study on the Bern area situated on the northern margin of the European Alps (Figure 2). For this region, we draw a map of the bedrock topography combining the results of a gravimetry survey in the region (Bandou, 2023a; Bandou et al., 2023) with information obtained through drillings. This map shows that an overdeepened trough or a tunnel valley system, referred to as the Aare main overdeepening (Schwenk et al., 2022a), is made up of two basins separated by a bedrock riegel, which itself is cut by one or multiple slot canyons. This

Deleted: An ensemble consisting of a riegel separating upstream and downstream basins has been considered as a classical feature of a landscape, which was repeatedly sculpted by glaciers during the past glaciations (Brocklehurst and Whipple, 2002; Brocklehurst et al., 2008; Cook and Swift, 2012; Steinemann et al., 2021). Observations from modern landscapes (see Figure 2 for examples in the Swiss Alps) have additionally shown that such bedrock swells or riegels may be cut by slot canyons or inner gorges (Montgomery and Korup, 2011; Steinemann et al., 2021), establishing a hydrological link between the upstream and downstream basins. These features were used as key information for invoking dissection by meltwater as an important erosional mechanism (Carter and Anderson, 2006; Steinemann et al., 2021). Although bedrock swells or riegels were reported as common features in overdeepenings (Gegg and Preusser, 2023), the occurrence of inner gorges or slot canyons (Figure 1) have only recently been disclosed (Bandou et al., 2023). It is the scope of this work to document such structures in an overdeepening and to discuss their importance for our understanding of how such depressions were formed. ...

Formatted: English (UK)

Formatted: English (UK)

Formatted: English (UK)

Formatted: English (UK)

Formatted: English (US)

Deleted: aimed at exploring

Formatted: English (UK)

Deleted: tunnel valleys or

Formatted: English (UK)

Deleted: 3a

Formatted: English (UK)

Deleted: structure

Formatted: English (UK)

Deleted: drilling

Formatted: English (UK)

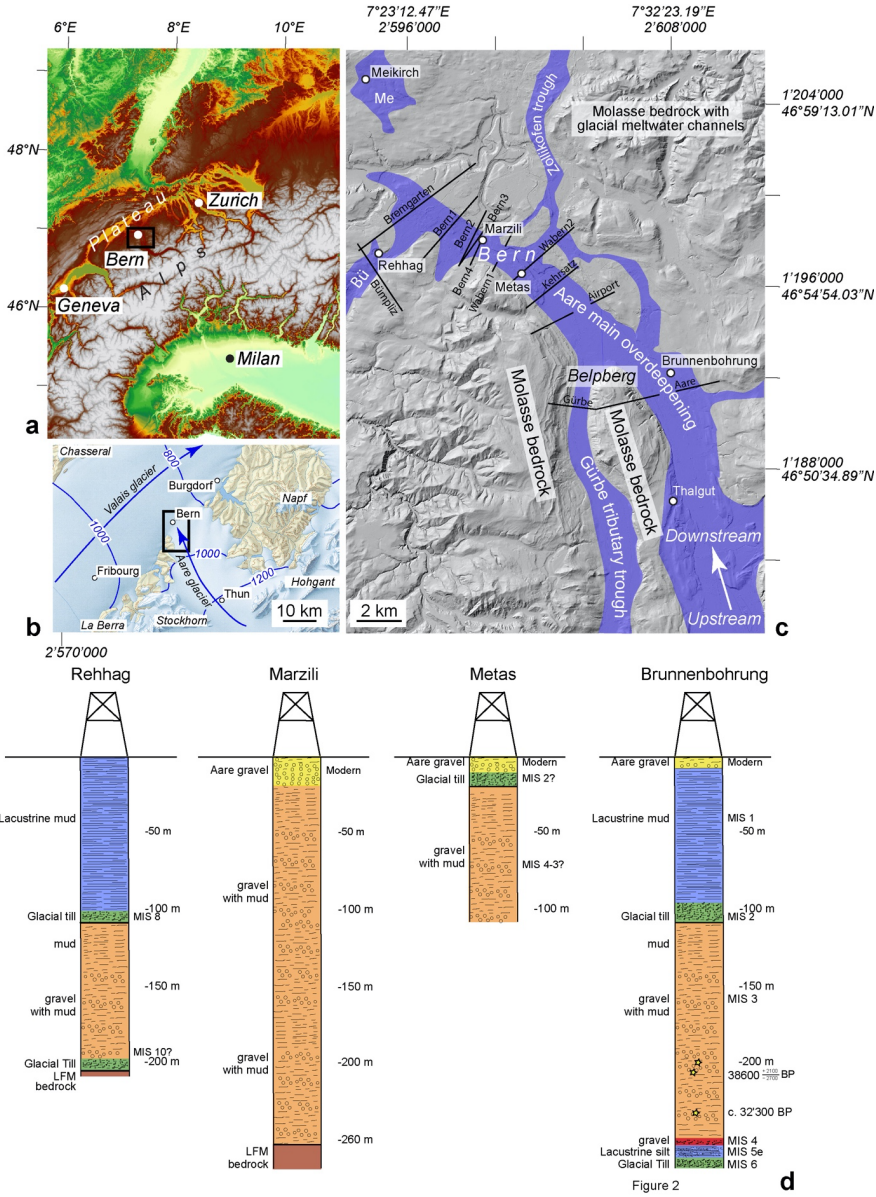
Deleted: 2022

Formatted: English (UK)

Formatted: English (UK)

177 structure has a similar geometry as [many](#) examples reported from [formerly glaciated landscapes](#)
 178 ([Brocklehurst and Whipple, 2002](#); [Brocklehurst et al., 2008](#)) and particularly from Alpine valleys,
 179 which points to similar processes resulting in their formation.

- Deleted: the
- Deleted: the
- Formatted: English (UK)
- Formatted: English (UK)



180

Figure 2: Local setting illustrating the a) Alpine arc (modified from Bandou et al., 2023) with latitudes and longitudes, b) the study area during the Last Glacial Maximum (LGM; map with isohypses of the glacier's surfaces taken from Bini et al., 2009), c) the surface geomorphology (2 m-SwissAlti3D DEM © swisstopo) together with the orientation of the Aare main overdeepening, taken from Reber and Schlunegger (2016), and d) information from drillings. The figure c) shows (i) the sections along which gravity data was collected (black lines; Bandou et al., 2022; 2023), and (ii) the sites (white circles) where sediments in drillings (Rehag; Schwenk et al., 2022a, b; Meikirch; Welten, 1982; Preusser et al., 2005; Schläfli et al., 2021; Brunnenbohrung: Kellerhals and Häfeli, 1984; Zwahlen et al., 2021) and exposures (Thalgut; Welten, 1982; 1988; Schlüchter, 1989; Preusser and Schlüchter, 2004) were either dated with various techniques, or where existing ages were reconfirmed by a subsequent analysis. Me=Meikirch overdeepening; Bü=Bümpliz trough. The numbers along the figure margin refer to the Swiss coordinate system (CH1903+) and are complemented with information on latitudes and longitudes. Panel d) presents the logs of key drillings. The Brunnenbohrung drilling was reconstructed from cuttings; the material at Metas and Rehag was cored (Geotest, 1997; Schwenk et al., 2022a), whereas the sedimentary log of the Marzili drilling is based on a combination of cuttings and gamma ray data (Gees, 1974). The log of the Brunnenbohrung is taken from Bandou et al. (2022).

2 Setting

2.1 Overdeepened troughs in the Bern area

The target overdeepening near Bern was sculpted by the Aare piedmont glacier with sources in the Central European Alps. From there, the Aare glacier flowed onto the Swiss Plateau (Figure 2a) over a distance of >20 km, and it merged with the Valais glacier north of Bern, at least during the Last Glacial Maximum (LGM) c. 20 ka ago (Figure 2b). Upstream of the city area of Bern, two bedrock depressions, referred to as the Gürbe tributary trough and the Aare main overdeepening (Figure 2c), form prominent basins. They are between c. 150 (Gürbe trough; Geotest, 1995) and >250 m deep (Aare main trough, Kellerhals and Häfeli, 1984), and several km wide (Bandou et al., 2022). Downstream of the city of Bern, the Aare main overdeepening splits into several distributary branches. Among these, the Bümpliz trough ('Bü' in Figure 2c) is the most prominent one with a depth >200 m (Schwenk et al., 2022a, b). The other depressions such as the Zollkofen trough are shallower and reach a depth of <150 m (Reber and Schlunegger, 2016). The study region also hosts the Meikirch overdeepening (labelled as 'Me' on Figure 3c), a nearly 200 m-deep trough (Dürst Stucki et al., 2010; Dürst Stucki and Schlunegger, 2003), which appears to be isolated from the rest of the overdeepening system (Reber and Schlunegger, 2016). Although the area between the northern termination of the Aare main overdeepening and the Meikirch trough is made up of exposed bedrock (Gerber, 1927), the possibility of a connection between both depressions via a narrow canyon, while quite unlikely according to Reber and Schlunegger (2016), cannot be completely ruled out. The Aare main overdeepening itself is the most prominent trough in the city area of Bern and has a maximum depth of nearly 250 m (Reber and Schlunegger, 2016).

2.2 Chronologic framework of overdeepening fill

The Quaternary fill of the Aare main overdeepening has been placed into the chronological framework of glacial advances onto the Swiss plateau during the past glaciations by previous authors. South of Bern, the Thalgut section (Figure 2c) disclosed the occurrence of pollen fragments embedded in a

Formatted: English (UK)

Deleted: Riegels and slot canyons in the Alpine valleys, and overdeepenings

Formatted: Font: Not Bold, Italic, English (UK)

Formatted: Justified

Deleted: Bedrock swells between neighboring basins are common features in previously glaciated landscapes and have been reported from various regions around the globe (

Deleted: They are particularly found in the European Alps (see Figure 2, for a few examples), and they have also been detected underneath active glaciers (Feigel et al., 2018;

Deleted: In the Alps, most of the bedrock swells occur at the base of valleys (Figure 2) and are dissected by inner gorges or slot canyons that connect the upstream with the downstream basin (Hantke and Scheidegger, 1973; Valla et al., 2009; Montgomery and Korup, 2011). In addition, the Alpine bedrock riegels have a geometry where the upstream s (... [11])

Formatted: English (UK)

Formatted: English (UK)

Formatted: English (UK)

Formatted: English (UK)

Deleted: 3b

Formatted: English (UK)

Deleted: channel

Deleted: 3c

Formatted: English (UK)

Formatted: English (UK)

Deleted: that

Formatted: English (UK)

Deleted:)

Deleted: kilometers

Formatted: English (UK)

Formatted: English (UK)

Deleted: channel

Deleted: 3c

Deleted:

(... [12])

Formatted: English (UK)

Formatted: English (UK)

Formatted: English (UK)

Deleted: ¶

(... [13])

Formatted: English (UK)

Formatted: English (UK)

Deleted: was ruled out (

Deleted: ,

Deleted:).

Formatted: English (UK)

Formatted: English (UK)

Formatted: English (UK)

255 lacustrine sequence at the base and near the top of the section (Schluchter, 1989). The pollen assemblage
256 at the base was assigned to the Holsteinian interglacial period (Welten, 1982; 1988; Schluchter, 1989;
257 Preusser and Schluchter, 2004), which either corresponds to MIS 9 (Roger et al., 1999) or MIS 11 (see
258 discussion in Preusser et al., 2011; Koutsodendris et al., 2012; and Schwenk et al., 2022a for discussion
259 of ages). The lacustrine sediments near the top of the same suite were assigned to MIS 5e (Welten,
260 1982; 1988; Schluchter, 1989). Approximately 6 km farther downstream of the Thalgut section, the
261 Brunnenbohrung drilling (Figure 2d) penetrated nearly the entire sedimentary sequence of the Aare
262 main overdeepening. Based on lithostratigraphic constraints and ¹⁴C ages established on organic
263 fragments, Kellerhals and Häfeli (1984) and subsequently Zwahlen et al. (2021) assigned an age
264 postdating MIS 6 to the entire succession. Farther north of Bern, Schwenk et al. (2022a) used the results
265 of feldspar luminescence dating to propose that the sedimentary suite penetrated by the Rehhag drilling
266 has an age of MIS 8 and older (Figure 2d). These ages are not precise enough to reconstruct in detail
267 the history of how and when the overdeepenings were formed, but they are consistent with the view
268 that the deep troughs in the Bern area were originally formed after the Middle Pleistocene Transition c.
269 800 ka ago (Schluchter, 2004) and thus during the same period when the U-shaped Alpine valleys were
270 carved (Häuselmann et al., 2007; Valla et al., 2011).

271 272 2.3 Lithological architecture of bedrock

273 The bedrock in the region comprises an amalgamated suite of Early Miocene Upper Marine Molasse
274 (UMM) sandstone beds south of Bern. Sedimentological analyses showed that these sediments were
275 deposited in a shallow marine, mostly coastal environment (Garefalakis and Schlunegger, 2019). In the
276 region north of Bern, the bedrock is made up of a Late Oligocene to Early Miocene suite of Lower
277 Freshwater Molasse (LFM) sandstones and mudstones (Isenschmid, 2019). These sediments were
278 deposited in a fluvial environment comprising channel fills and floodplains made up of sandstones and
279 mudstones, respectively (Platt and Keller, 1992; Isenschmid, 2019). The bedding of the sediments and
280 the contact between the UMM and the LFM gently dips towards the south by c. 10° (Isenschmid, 2019),
281 with the consequence that south of Bern, the base of the Aare main overdeepening often consists of
282 LFM deposits, while most of the upper part of the overdeepening is laterally bordered by bedrock made
283 up of UMM. In addition, it has been postulated that the UMM sediments have a lower erodibility than
284 the underlying LFM unit, based on the observation that the UMM forms a cap rock in the region
285 (Isenschmid, 2019). Finally, Isenschmid (2019) documented that the Molasse bedrock beneath the Bern
286 city area is dissected by left-lateral faults that strike NW-SE, offering zones of mechanical weaknesses.

287 288 2.4 Lithological architecture of overdeepening fill

289 Detailed information on the lithologic architecture of the overdeepening fill is available from a few
290 drillings only (Figure 2d). South of Bern, the >250 m-thick succession at the Brunnenbohrung site starts

Moved (insertion) [4]

Formatted: English (UK)

Deleted: originally

Formatted: English (UK)

Formatted: English (UK)

Formatted: English (UK)

Formatted: English (UK)

Deleted: might consist

Formatted: English (UK)

Deleted: of the UMM.

Formatted: English (UK)

Moved down [5]: 3 → Dataset and Methods

Deleted: 3.1 → Compilation

Formatted: English (UK)

296 with a few meters of till (possibly MIS 6), yet the drilling did not reach the bedrock. The till is overlain
297 by a several m-thick lacustrine silt (possibly MIS 5e) and a >100 m-thick sequence made up of
298 fluviolacustrine gravel, dated to MIS 3 based on ¹⁴C concentrations in organic matter (Kellerhals and
299 Häfeli, 1984). The topmost 100 m-thick suite comprises a till at its base (possibly MIS 2) and a
300 monotonous succession of lacustrine mud topped by a fluvial gravel. Farther north, the Metas drilling
301 penetrated a 110 m-thick sequence without reaching the bedrock (Geotest, 1997). It starts with a c. 90
302 m-thick suite made up of mud and sand layers, which contain isolated clasts. These sediments were
303 most likely deposited in a proglacial lake. It is overlain by a till (MIS 2?) and finally by a c. 15 m-thick
304 proglacial gravel (Geotest, 1997). A similar sedimentologic architecture, based on cutting and gamma
305 ray data, was also inferred for the Quaternary suite penetrated by the Marzili drilling situated in the city
306 area of Bern (Gees, 1974). Finally, the Rehhag drilling, which was sunk into the Bümpliz tributary
307 trough and which reached the bedrock (Schwenk et al., 2022a), unravelled a 210 m-thick succession of
308 Quaternary sediments. The Quaternary suite starts with a few m-thick till, which is overlain by a c. 100
309 m-thick sequence of mud, gravel and sand layers. A second till was identified at a drilling depth of 103
310 m. It is overlain by a succession of mud with isolated pebbles, deposited in a proglacial lake. Apparently,
311 the Quaternary successions are spatially highly heterogeneous as disclosed by the drillings, but they all
312 record the same depositional setting as the sediments were most likely deposited in a glacio-lacustrine
313 environment (e.g., Schwenk et al., 2022a).

314 315 2.5 Density of Molasse bedrock and Quaternary sediments

316 Data on the bulk density of the Molasse bedrock and the overlying Quaternary sediments is crucial for
317 interpreting gravimetric datasets (Kissling and Schwendener, 1990). For the Bern region, Bandou et al.
318 (2022) used the results of a Nettleton profile across the Belpberg mountain (that is underlain by Molasse
319 bedrock, Figure 2c) to assign a bulk density of 2500 kg/m³ to the Molasse units (Figure 2c). This is a
320 substantially higher value than the bulk densities between 2150 and 2000 kg/m³, which have been
321 determined for the basal part and the top sequences of the Quaternary suites in the Aare main
322 overdeepening, respectively. These density values were measured with a multi sensor core logger on
323 the core of the Rehhag drilling (Schwenk et al., 2022a) and obtained through 3D gravity modelling
324 along several profiles in the Bern area (Bandou et al., 2022; 2023a). The results showed that the bulk
325 densities of the Quaternary sediments depend less on the lithological architecture of the material or the
326 depositional environment in which the sediments were deposited. Instead, they are primarily a function
327 of the maximum depth of the overdeepening fill and the number of glaciations, during which the
328 Quaternary sediments were compacted under a thick glacial cover (Bandou et al., 2023).

Deleted: data

Formatted: Font: Not Italic, English (UK)

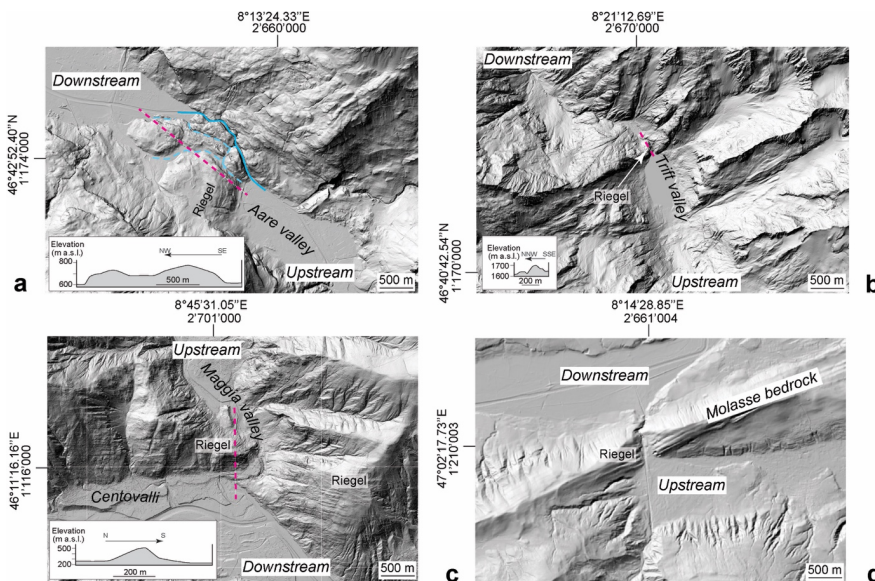
Formatted: Font: Not Italic, English (UK)

333 2.6 Riegels and slot canyons in Alpine valleys

334 Bedrock swells between neighbouring basins are common features in previously glaciated landscapes
335 (Anderson et al., 2006; Alley, 2019). They are common in the European Alps (see Figure 3, for a few
336 examples), and they have also been detected underneath active glaciers (Feiger et al., 2018; Nishiyama
337 et al., 2019). In the Alps, most of the bedrock swells cross the thalweg of valleys (Figure 3) and are
338 dissected by inner gorges or slot canyons that connect the upstream with the downstream basin (Hantke
339 and Scheidegger, 1973; Valla et al., 2010; Montgomery and Korup, 2011). In addition, Alpine bedrock
340 riegels have a geometry where the upstream stoss side is flatter than the downstream lee side (insets of
341 Figure 3). This is particularly the case for the swells in (Figure 3): the Aare valley (Figure 3a: dip of
342 stoss side and lee sides <5° and >6°, respectively; Hantke and Scheidegger, 1973), the Trift valley
343 (Figure 3b: c. 30° versus 40°; Steinemann et al., 2021), and the Maggia valley (Figure 3c: 6° versus
344 40°). Bedrock riegels and slot canyons are also found on the foreland plateau adjacent to the Alps such
345 as the example east of Lucerne (Figure 3d), yet their geometric expressions are less well-developed. In
346 this work, we will document that the overdeepening beneath the city of Bern shares the same geometric
347 properties as the ensemble of bedrock riegels and slot canyons in Alpine valleys.

Formatted: English (UK)

Formatted: English (UK)



348 Figure 3

349 Figure 3: Hillshade 2 m-SwissAlti3D DEM (© swisstopo) illustrating examples in Alpine valleys where
bedrock riegels separate overdeepened basins situated farther upstream and downstream. The
insets illustrate topographic sections across the riegels, and the arrows display the flow direction
of the glaciers during a glaciation. The coordinates refer to the Swiss coordinate system
(CH1903+). Longitudes and latitudes are also indicated.

350 **3 Dataset and Methods**

351 The bedrock topography beneath the city area of Bern was already reconstructed in 2010 and then

352 updated in 2016, based on information from thousands of drillings publicly available on the Geoportal

353 of the Canton Bern (see Dürst Stucki et al. (2010), and Reber and Schlunegger (2016), respectively).

354 Since these drillings primarily penetrated the entire Quaternary sequence down to the bedrock at the

355 lateral margins of the Aare main overdeepening, we consider the bedrock topography model of Reber

356 and Schlunegger (2016) for the shallow parts of the trough as accurate. Yet detailed reconstructions of

357 the deeper, central part of the overdeepening were hindered due to a lack of information from deep

358 drillings at that time (Reber and Schlunegger, 2016). Here, we benefit from the results of a recent gravity

359 survey conducted in the city area of Bern (Bandou et al., 2022; 2023; Bandou, 2023a) and information

360 from new drillings >50 m deep. We proceeded through compiling, as a first step, the publicly available

361 gravity data. We re-processed them to provide information about the spatial pattern of the gravity signal,

362 either from the bedrock topography beneath the overdeepening fill (section 3.1) or from the

363 overdeepening fill itself (section 3.2). Using these data along with the results from modelling conducted

364 by Bandou et al. (2023), we reconstructed a map outlining the general thickness distribution of the

365 Quaternary sediments (section 3.3). This was then used as the basis to update the existing bedrock

366 topography model of Reber and Schlunegger (2016), thereby incorporating data from >100 drillings

367 that penetrated >50 m into the subsurface (section 3.4).

368

369 *3.1 Assessing the gravity signal of the bedrock topography beneath the overdeepening*

370 We compiled the gravity data collected by Bandou (2023a) and combined them with data archived in

371 the Gravimetric Atlas of Switzerland by Swisstopo (Olivier et al., 2008; 2011). From this dataset, we

372 calculated the Bouguer anomaly values (see Bandou et al., 2023, for references to the methodological

373 papers) using the density of the Molasse bedrock (2500 kg/m³) instead of the standard density of 2670

374 kg/m³ that is conventionally used for Bouguer anomaly corrections. We then draw the isogals (contour

375 lines of equal Bouguer anomaly values) using the Golden Software Surface licensed to Swisstopo. This

376 map was used to infer the general shape of the bedrock topography beneath the overdeepening fill. In

377 particular, deviations of the isogals from the long-wavelength trend can serve as *a-priori* constraints for

378 reconstructing the course and geometry of the bedrock outlining the overdeepening.

379

380 *3.2 Assessing the gravity signal of the Quaternary sediments overlying the overdeepening*

381 Subtracting the Bouguer anomalies values measured along a profile from the regional gravity field along

382 the same profile yields what is referred to as the residual gravity anomaly. The related values provide

383 information about a near-surface body or structure with a bulk density different from that of the

384 surrounding bedrock (Kissling and Schwendener, 1990). Bandou et al. (2022; 2023) used this concept

385 to determine the gravity signal of the Quaternary sediments overlying the Molasse bedrock. They

Formatted ... [14]

Deleted: underneath

Formatted ... [15]

Deleted: retrieved

Deleted: that is

Deleted: from

Formatted ... [16]

Formatted ... [17]

Formatted ... [18]

Deleted: ..

Deleted: ;

Deleted: ,

Deleted:). Whereas such information yielded highly ... [22]

Formatted ... [19]

Formatted ... [20]

Formatted ... [21]

Formatted ... [23]

Deleted: ,

Deleted:),

Formatted ... [24]

Formatted ... [25]

Deleted: details for the

Formatted ... [26]

Deleted: and thus

Deleted: Aare main

Deleted: have been thwarted because of

Deleted: drilling

Formatted ... [27]

Formatted ... [28]

Formatted ... [29]

Formatted ... [30]

Deleted: .

Formatted ... [31]

Deleted: of

Deleted: (Bandou et al., 2023; Figure 3c).

Formatted ... [32]

Formatted ... [33]

Deleted: Bandou et al. (2023) measured

Deleted: gravity

Deleted: along 10 sections (black lines in Figure 3c). ... [36]

Deleted: yielding a

Formatted ... [34]

Formatted ... [35]

Formatted ... [37]

Deleted: value at each site where gravity data was collected.

Formatted ... [38]

440 proceeded by calculating the residual gravity anomaly values along 10 profiles perpendicular to the
 441 inferred course of the Aare main overdeepening (black lines in Figure 2c). Note that because the
 442 Quaternary deposits have a lower bulk density than the Molasse bedrock, the occurrence of such
 443 deposits results in a negative residual gravity anomaly (Kissling and Schwendener, 1990). Accordingly,
 444 a larger bulk mass of Quaternary sediments yields a stronger (and thus a more negative residual
 445 anomaly) signal than a fill with less Quaternary material (Kissling and Schwendener, 1990; Bandou et
 446 al., 2022). Following this concept, we compiled the residual anomaly data from Bandou et al. (2023)
 447 for each gravity profile and drafted a contour map where each line displays the same residual anomaly
 448 value. This map was drawn by hand, thereby considering the *a-priori* information about the orientation
 449 of the Aare main overdeepening (Reber and Schlunegger, 2016).

451 3.3 Estimating the thickness of Quaternary sediments based on gravity data

452 Residual gravity anomaly values can be converted to thicknesses of Quaternary sediments through
 453 modelling, provided that *a-priori* data is available (Kissling and Schwendener, 1990). This includes
 454 information on: (i) density contrasts between the Molasse bedrock and the Quaternary fill, (ii) depths
 455 of bedrock encountered in drillings, and (iii) an already existing bedrock topography model (in our case
 456 the bedrock topography model of Reber and Schlunegger, 2016). Bandou et al. (2023) used a 3D gravity
 457 software referred to as PRISMA (Bandou, 2023b) to implement this approach, modelling the residual
 458 gravity anomalies along six profiles (Figure 5b) where the aforementioned *a-priori* data is well
 459 constrained. Note that upon using PRISMA, the geometry of the overdeepening fill was approximated
 460 by Bandou et al. (1922, 1923) through multiple right-handed prisms oriented as perpendicularly as
 461 possible to the profile of interest (Nagy, 1966; Banerjee and Das Gupta, 1977). We compiled the results
 462 of the PRISMA modelling presented by Bandou et al. (2022, 2023) to draw a map displaying the
 463 thickness distribution of Quaternary sediments overlying the Aare main overdeepening. When creating
 464 this map, we considered that a trend towards smaller or larger negative residual anomalies indicates a
 465 thinning or thickening of the Quaternary sediments, respectively (Kissling and Schwendener, 1990;
 466 Bandou et al., 2023). The difference between the elevation of the modern topography and the thickness
 467 of the Quaternary sediments returns a map displaying the bedrock topography.

469 3.4 Combining the results of the gravity survey with drilling data to reconstruct the details of the 470 bedrock topography

471 We updated the bedrock model of Reber and Schlunegger (2016) with information about the general
 472 shape of the overdeepening retrieved through gravity modelling outlined above, and we additionally
 473 considered the information of >100 drillings that were sunk >50 m deeply into the subsurface during
 474 the past years. Similar to Reber and Schlunegger (2016), we manually drew the isohypses of the
 475 bedrock, inferring that changes in the orientation of the contour lines and the depths of the bedrock were

Formatted ... [39]
 Deleted: and thus the overdeepening fill has ... [40]
 Formatted ... [40]
 Deleted: Oligo-Miocene sediments forming the bedro ... [41]
 Formatted ... [42]
 Deleted: Quaternary sediments overlying an overdeep ... [43]
 Formatted ... [44]
 Deleted: (Figure 4a)
 Formatted ... [45]
 Deleted: 2
 Formatted ... [46]
 Deleted: general shape
 Formatted ... [47]
 Deleted: the
 Formatted ... [48]
 Deleted: topography?
 Formatted ... [49]
 Deleted: were
 Formatted ... [51]
 Deleted: , Bandou et al. (2023) reconstructed the cross ... [52]
 Formatted ... [53]
 Deleted: a 3D gravity software referred to as PRISMA ... [54]
 Formatted ... [55]
 Deleted: to predict the gravity effect of a given struct ... [56]
 Formatted ... [57]
 Deleted: . It bases on an analytical solution by ... (Nag ... [58]
 Formatted ... [59]
 Deleted: an overdeepening fill. Upon applying this model,
 Deleted: (2023) particularly considered geophysical a ... [61]
 Deleted: reconstruct the general course of the isohyps ... [63]
 Formatted ... [60]
 Formatted ... [62]
 Deleted: less
 Formatted ... [65]
 Deleted: points towards
 Formatted ... [66]
 Deleted: shallowing
 Formatted ... [67]
 Deleted: bedrock
 Formatted ... [68]
 Deleted: 2023).
 Formatted ... [69]
 Deleted: 3.
 Formatted ... [70]
 Deleted: used
 Deleted: existing
 Deleted: topography map
 Deleted: as a basis where the isohyps were original ... [74]
 Formatted ... [71]
 Formatted ... [72]
 Formatted ... [73]
 Formatted ... [75]
 Deleted: the
 Formatted ... [76]
 Deleted: data by Bandou et al. (2023) (Figure 4),
 Formatted ... [77]
 Deleted: (Figure 5).
 Formatted ... [78]
 Deleted: draw
 Formatted ... [79]
 Deleted: by hand thereby
 Formatted ... [80]

602 gradual. We finally combined the map displaying the geometry of the bedrock beneath the
 603 overdeepening with the elevation data provided by the 2 m-SwissAlti3D DEM (based on LIDAR data
 604 of swisstopo) to present the shape of the bedrock topography as shaded relief.

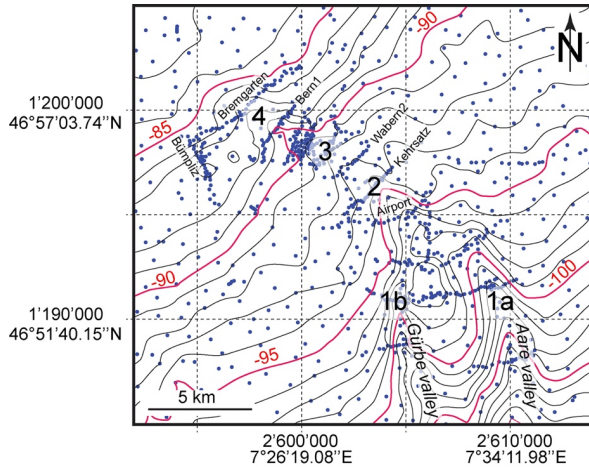


Figure 4

Figure 4: Bouguer anomalies, calculated with the density of the Molasse bedrock (2500 kg/m^3). The blue dots are gravity data taken from the Gravimetric Atlas of Switzerland (Olivier et al., 2008; 2011; swisstopo) and from Bandou (2023a). The isogals, indicated in mGal, illustrate the general gravity trend in the region and deviations thereof. 1a and 1b are sites located in the Aare and Gürbe valleys, respectively. These are the locations where the isogals have the largest deflections from the large-wavelength trend. Farther to the N (site 2) and then to the NW, the deflections decrease, reaching the lowest values at site 3. They increase again towards site 4 and then fade towards the NW. The figure also shows the locations of the gravity profiles presented in Bandou (2022) and Bandou et al. (2023). The grid corresponds to the Swiss coordinate system (CH1903+). Longitudes and latitudes are also indicated.

4 Results

4.1 Isogals and gravity signal of the bedrock topography beneath the overdeepening

The isogals calculated with the density of bedrock (2500 kg/m^3) clearly depict the general gravity trend, which is characterized by a continuous SE-directed increase of the Bouguer anomaly values from -85 mGal in the NW to -105 mGal towards the SE (Figure 4). Note that a more negative value implies a stronger gravity anomaly. The isogals generally strike SW-NE, reflecting the orientation of European continental lithosphere, which gently dips beneath the Alpine orogen. However, and most importantly in our context, the isogals also deviate from this pattern by being deflected towards the NW, where we expect the occurrence of the Gürbe tributary trough and the Aare main overdeepening. This anomaly (or deflection) has indeed the largest amplitudes of $>4 \text{ mGal}$ and $>3 \text{ mGal}$ beneath the Aare (location 1a on Figure 4) and Gürbe valleys, respectively (location 1b). This indicates that the depth of the overdeepened trough is greatest there. Farther to the NW, the amplitude of the deflection decreases from approximately 3 mGal at site 2 (between Airport and Kehrsatz) to $<1 \text{ mGal}$ at site 3 (Figure 4),

Deleted: underneath

Formatted: English (UK)

Deleted: offered

Formatted: English (UK)

Deleted: We finally used this map as a basis to draw the cross-sections displayed in Figures 6 and 7.

Formatted: English (UK)

Formatted: Font: Italic, English (UK)

Formatted: English (UK)

Deleted: Patterns

Formatted: English (UK)

625 [suggesting a shallowing of the bedrock trough and thus the occurrence of a swell \(or riegel\). From there,](#)
 626 [the amplitude increases again at site 4 as the trough appears to deepen once more. after which the](#)
 627 [anomaly fades farther to the NW.](#)
 628

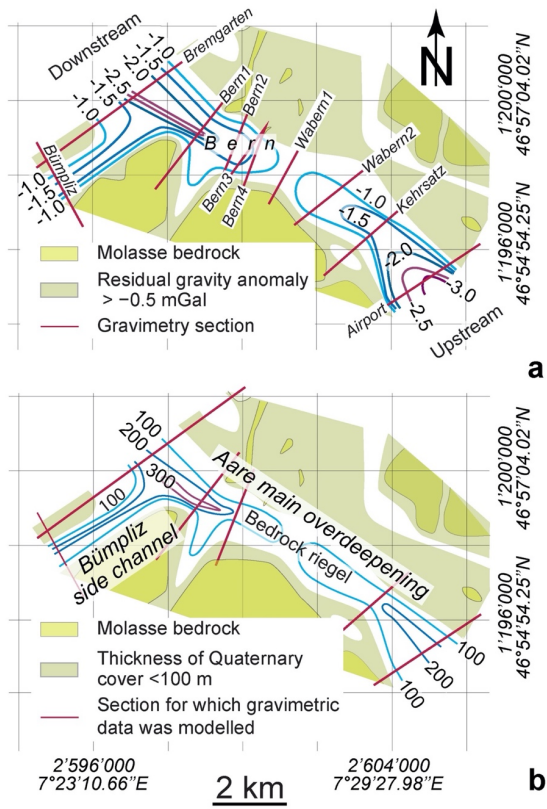


Figure 5

629

Figure 5: Residual gravity anomalies, representing the gravity signal of Quaternary sediments, and inferred thicknesses of Quaternary deposits. a) The contour lines of the residual gravity signals (mGal) caused by the Quaternary fill of the Aare main overdeepening are mainly based on gravity surveys along 10 sections (red lines; Bandou et al., 2023). Here, more negative values imply a greater signal caused by the bulk mass of Quaternary sediments overlying the overdeepened trough (Kissling and Schwendener, 1990; Bandou et al., 2022). b) Spatial distribution of Quaternary sediments, here expressed by the related thicknesses. These are mainly based on the results of gravity modelling, where Quaternary mass and its spatial distribution was forward modelled until a best-fit between the modelled and observed gravity signals of the Quaternary mass overlying the overdeepened trough was reached (Bandou, 2023; Bandou et al., 2023). Note that only the residual gravity anomalies of the Airport, Kehrsatz, Bern2, Bern1, Bremgarten and Bümpliz sections were modelled by Bandou et al. (2023). The grid refers to the Swiss coordinate system (CH1903+). Longitudes and latitudes are also indicated.

4.2 Gravity signals of the Quaternary sediments overlying the overdeepening

The residual gravity anomalies, which correspond to the gravity signal of the Quaternary sediments, reveal the same pattern as the isogals where the Bouguer anomaly values were calculated with the bedrock density of 2500 kg/m³. For the section across the Gürbe and Aare valleys (Figure 2c), Bandou et al. (2022; 2023) showed that the Quaternary fill of the Aare main overdeepening results in a gravity signal that ranges between c. -4.0 and -0.5 mGal. In addition, they showed that this signal changes from upstream to downstream. In particular, along the Gürbe-Aare transect (Figure 2c), which also crosses the Belpberg mountain ridge made up of Molasse bedrock, the strength of the signal ranges from c. -2.9 mGal in the Gürbe valley to c. -4.1 mGal in the Aare valley (Bandou et al., 2022). Farther downstream, the residual anomaly values and thus the signal of the overdeepening fill decreases, where the corresponding values change from c. -3.0 mGal (Airport profile) to approximately -1.5 and finally c. -1.0 mGal along the Kehrsatz and Wabern2 profiles, respectively (Figure 5a). The weakest signals with values between c. -0.5 mGal and -1 mGal were reported for the Wabern1 profile (Bandou et al., 2023; Figure 5a). This suggests a decrease in the mass of Quaternary sediments approaching Wabern1, most likely due a shallowing of the bedrock forming a riegel in this area. Farther downstream, the gravity signal of the Quaternary fill increases again and reaches values between c. -1.0 and c. -2.0 mGal along the Bern sections, and then approximately -2.5 mGal along the Bremgarten section c. 2 km farther downstream. This points towards an increase in the Quaternary mass and thus towards a deepening of the trough in this direction. The residual anomaly data thus clearly depict the course of the Aare main overdeepening, which strikes SE-NW in the city area of Bern (Figures 2c, 5a). Towards the NW margin of the study area, a second overdeepening referred to as the Bümpliz tributary trough (Schwenk et al., 2022a) strikes SW-NE and converges with the Aare main overdeepening NW of Bern. The gravity signal of the Bümpliz sedimentary fill is less and reaches a value of c. -1.5 mGal (Figure 5a; Bandou et al., 2023). Finally, the upstream side of the inferred bedrock riegel dips gentler than the downstream side, which is twice as steep: on the stoss side, the residual gravity anomalies change from <-2.5 mGal to >-1.0 mGal over a downstream distance of c. 4 km whereas on the lee side, the same change in the gravity signal occurs over only 2 km. Given that the residual gravity signal is a direct response of the

- Deleted: ¶ ... [82]
- Formatted: Font: Not Italic, English (UK)
- Formatted: English (UK)
- Deleted: residual
- Deleted: anomaly
- Formatted: English (UK)
- Formatted: English (UK)
- Deleted: the gravity signal of the Quaternary fill has a ... [83]
- Formatted: English (UK)
- Deleted: .
- Deleted: 3c
- Formatted: English (UK)
- Formatted: English (UK)
- Deleted: a
- Deleted: (Belpberg)
- Deleted: corresponding maximum residual anomalies
- Formatted: English (UK)
- Formatted: English (UK)
- Formatted: English (UK)
- Deleted: signals
- Deleted: ¶ ... [84]
- Formatted: English (UK)
- Formatted: English (UK)
- Deleted: 4a
- Deleted: lowest residual anomaly signal
- Formatted: English (UK)
- Formatted: English (UK)
- Deleted: 3a).
- Formatted: English (UK)
- Deleted: related to
- Formatted ... [85]
- Deleted: collected along the aforementioned gravity sections
- Formatted: English (UK)
- Deleted: 3c, 4a
- Formatted: English (UK)
- Deleted: side channel
- Formatted: English (UK)
- Deleted: 2022b
- Formatted: English (UK)
- Deleted: 4a
- Formatted: English (UK)
- Deleted: ¶ ... [86]
- Deleted: which becomes 100 m and possibly less (Fig ... [87]
- Formatted: English (UK)
- Formatted ... [88]

747 bulk mass of Quaternary sediments overlying the Molasse bedrock (see section 4.2), and thus their
748 volume supposing a lower density than the Molasse bedrock (see next section and Bandou et al., 2022;
749 2023), the differences in the upstream and downstream gradients of the residual gravity anomaly values
750 disclose the contrasts in the dip angles of the bedrock topography.

752 4.2 Thickness of Quaternary sediments

753 Available drilling information shows that the Quaternary fill in the Bern region generally consists of an
754 alternation of gravel, sand and mud (Figure 2d), which have a bulk density that ranges from 2150 kg/m³
755 for material at the base of the overdeepening fill, to 2000 kg/m³ for the sediments towards the top. Based
756 on a sensitivity analysis where the gravity response to different densities for the Quaternary sediments
757 was evaluated, Bandou (2023a) and Bandou et al. (2022, 2023) could exclude the possibility that the
758 Bouguer anomaly and residual anomaly patterns displayed in Figures 4 and 5a could be explained by
759 spatial differences in the sedimentary architecture of the Quaternary fill. For instance, the low residual
760 gravity anomalies displayed in the region of the Wabern2 profile (Figure 5a) would require an
761 amalgamation of highly compacted glacial till. However, this is not consistent with the stratigraphic log
762 of the core drilled at Metas (Figure 2d), which is made up of an alternation of sand, mud and gravel that
763 was most likely deposited in a lacustrine environment. Instead, we prefer a perspective where the pattern
764 of residual gravity anomaly values reflects spatial variations in the thickness of the Quaternary
765 sediments. Accordingly, the thickest Quaternary suite can be found upstream and downstream of Bern
766 (Figure 5b), where the Aare main overdeepening is between 4 and 5 km wide and >200 m deep,
767 consistent with drilling information (Bandou et al., 2023). In the city area of Bern, however, the main
768 trough tends to become shallower. This is indicated by the thickness of the Quaternary sediments
769 reaching 100 m and possibly less (Figure 5b). The thickness of the Quaternary sediments filling the
770 trough then increases again farther downstream.

772 4.3 The consideration of deep drillings discloses the occurrence of slot canyons

773 The reconstructed bedrock topography of the target region reveals a complex pattern (Figure 6), which
774 can be described as a bedrock riegel that is dissected by multiple, partly anastomosing slot canyons or
775 inner gorges (Bandou et al., 2023). At this stage, we cannot precisely reconstruct the number of the
776 inferred canyons because we lack a high-resolution database of deep drillings (Figure 6). Yet, the
777 discrepancy between (i) a relatively low gravity signal particularly between the Wabern2 and the Bern
778 sections (Figure 5a) and (ii) drillings that reached the bedrock at much deeper levels >200 m below the
779 surface (Figures 6) can only be resolved by invoking the occurrence of a plateau at shallow elevations
780 that is dissected by one or multiple slot canyons (Figure 7). These gorges are up to 150 m deep and may
781 connect the overdeepened basins upstream and downstream of the city area of Bern. In particular, south
782 of Bern along the Aare profile (Figures 2b and 8a), the Aare main overdeepening has a cross-section

Deleted: ,
Formatted: English (UK)
Formatted: English (UK)

Formatted: English (UK)
Formatted: English (UK)
Deleted: 5
Formatted: English (UK)
Deleted: 5
Formatted: English (UK)
Deleted: (Figure 6)
Formatted: English (UK)
Deleted: 4a
Deleted: several
Formatted: English (UK)
Deleted: that are
Formatted: English (UK)
Formatted: English (UK)
Deleted: 5,
Formatted: English (UK)
Deleted: .
Deleted: appear to
Formatted: English (UK)
Formatted: English (UK)
Deleted: 3b
Deleted: 7a
Deleted: is U-shaped in
Formatted: English (UK)
Formatted: English (UK)
Formatted: English (UK)

796 ~~that~~ displays two ~~superimposed~~ levels of U-shapes, each of which with steep lateral flanks and a flat
797 base. While the upper flat base occurs at an elevation of c. 450 m a.s.l., the lower flat contact to the
798 bedrock is situated at c. 250 m a.s.l. and thus approximately 200 m deeper than the upper level (Bandou
799 et al., 2022). Approximately 5 km farther downstream along the Airport section (Figures ~~2b, 8b~~), the
800 cross-sectional geometry of the Aare main overdeepening maintains its generally U-shaped geometry
801 with a base at an elevation between 200 and 250 m a.s.l. There, the base of the overdeepening appears
802 less flat than farther upstream, but we acknowledge that the density of ~~deep~~ drillings in the region
803 (Figure ~~6~~) and the resolution of the gravity data (Figure ~~5a~~, Bandou et al., 2023) is not high enough to
804 fully support this comparison. Upon approaching the city area of Bern, the base of the bedrock becomes
805 shallower and appears to evolve towards a plateau particularly between the Kehrsatz and Bern2 sections
806 (Figures ~~6, 7, 8c~~, d and e). This plateau is situated at an elevation of c. 400 m a.s.l. (dashed lines on
807 Figure ~~8~~) and dissected by multiple slot-canyons, ~~as evidenced by drillings reaching depths down to c.~~
808 ~~300 m a.s.l. and even lower elevations, yet the canyons remain undetected by the gravity survey. This~~
809 ~~implies that the canyons must be cutting~~ up to 150 m deep ~~below the plateau at c. 400 m a.s.l. and that~~
810 ~~they are~~ too narrow to be detected by the gravity survey (Bandou al., 2023). Farther to the Northwest
811 reaching the terminal part of the Aare main overdeepening (Figure ~~2b~~), the trough widens again and
812 gives way to a relatively deep basin where the deepest part occurs at an elevation of ~~almost~~ 300 m a.s.l.
813 (Figures ~~6, 8f~~). This terminal basin appears to be connected with the Bümpliz ~~tributary trough~~ farther
814 to the SW. Yet the density of drillings is too low (Figure ~~6~~) to determine whether a possible bedrock
815 swell separates the Aare main overdeepening from the Bümpliz tributary ~~trough~~ (Figure ~~2b~~).

- Deleted: and
- Formatted: English (UK)
- Formatted: English (UK)
- Formatted: English (UK)
- Deleted: 3b, 7b
- Formatted: English (UK)
- Formatted: English (UK)
- Deleted: 5
- Deleted: 4a
- Formatted: English (UK)
- Formatted: English (UK)
- Deleted: 5,
- Deleted: 7c
- Formatted: English (UK)
- Formatted: English (UK)
- Deleted: 7
- Formatted: English (UK)
- Formatted: English (UK)
- Deleted: some of which are
- Deleted: and
- Formatted: English (UK)
- Formatted: English (UK)
- Deleted: 3b
- Formatted: English (UK)
- Formatted: English (UK)
- Deleted: and possibly even deeper
- Deleted: 5, 7f
- Deleted: side channel
- Formatted: English (UK)
- Formatted: English (UK)
- Formatted: English (UK)
- Deleted: 5
- Formatted: English (UK)
- Deleted: channel
- Deleted: 3b
- Formatted: English (UK)
- Formatted: English (UK)

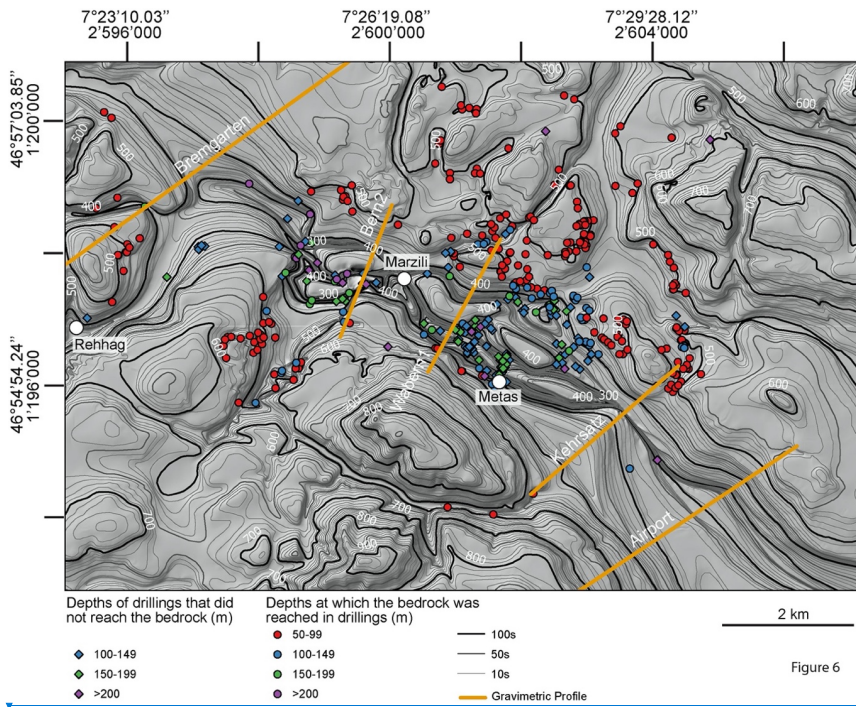


Figure 6: Hillshade DEM, illustrating the bedrock topography of the Bern area, together with deep drillings that either reached the bedrock (circles) or that ended in Quaternary sediments (diamonds). The shallow drillings (<50 m) are not displayed on this map since the number is too large (more than 1000, please see Reber and Schlunegger, 2016). The isohypses were drawn for every 10 m. The coordinates along the figure margin refer to the Swiss coordinate system (CH1903+). The sections shown on this map are used to illustrate the cross-sectional geometry of the overdeepening beneath Bern (see next figures).

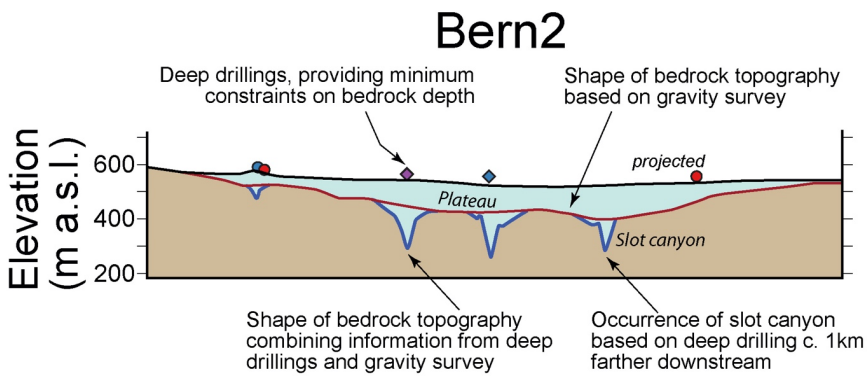
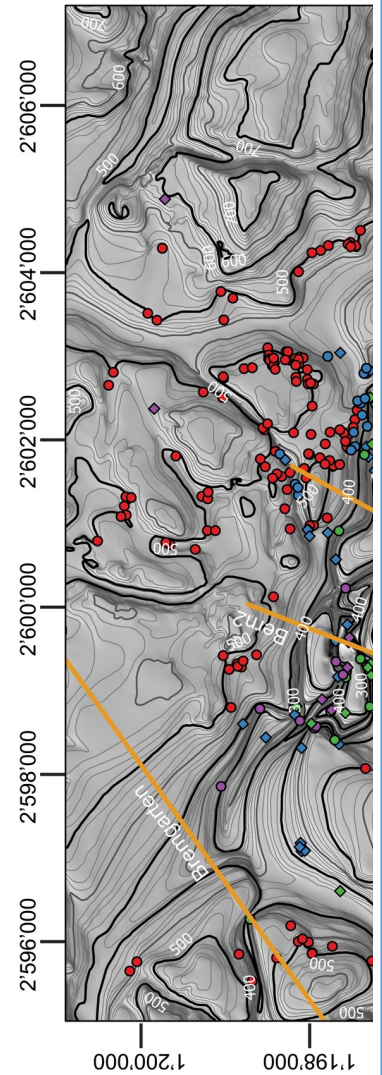


Figure 7



Deleted:

Formatted: English (UK)

Formatted: English (UK)

Deleted: 5

Deleted: meters

Figure 7: Example that illustrates how we proceeded upon reconstructing the bedrock topography beneath Bern. We started with the general shape of the bedrock topography using the gravity signal of the bulk Quaternary mass as a basis (red line, and Figure 5b). Information from drillings >50 m deep (circles and diamonds; see Figure 6 for explanation of colors) allowed then to reconstruct the course and geometry of the slot canyons (blue line). The mass of their Quaternary fill is too low to be identified by the gravity survey. This is the case because the strength of a gravity signal decays exponentially with depth (see also Bandou et al., 2023, for further explanations).

836

837 **5 Discussion**

Formatted: English (UK)

838 *5.1 Limitations upon reconstructing the bedrock topography model*

Deleted: 5.1

839 The inferred existence of a bedrock riegel and slot canyons below Bern is based on two features: (i)
840 gravimetric data showing a relatively low negative anomaly, which we interpret as a relatively low
841 depth to bedrock in the Bern city area, and (ii) previous borehole logs that show a much greater drilled
842 depth to bedrock. Indeed, the combination of deep bedrock detected from borehole data in an area of
843 otherwise characterized by shallow bedrock, as imaged by gravimetry, suggests that the canyons must
844 extend deeply while remaining highly confined in order to stay below the spatial resolution of the
845 gravimetry method. However, we acknowledge that no direct drilling evidence confirms the presence
846 of such a riegel. Nevertheless, the contour lines of the Bouguer anomaly values, calculated using a
847 density of bedrock (2500 kg/m³), indicate that the target overdeepening is generally broad and deep
848 upstream of Bern, shallow beneath the city, and then narrows and deepens downstream of it (Figure 4).
849 In addition, gravity data collected at 10 gravity stations along the Bern2 profile does point towards the
850 occurrence of a residual anomaly signal with a short wavelength beneath the main large-wavelength
851 residual gravity anomaly (Figures S1a and S1b in the Supplement). Indeed, using the results of 3D
852 gravity modelling, Bandou et al. (2023) considered the anomaly with the large wavelength as the gravity
853 response of the Quaternary fill overlying the bedrock riegel, whereas the short-wavelength anomaly
854 beneath it illustrates the possible occurrence of a slot canyon, filled by Quaternary sediments (Figure
855 S1c in the Supplement). Further slot canyons could not be identified upon modelling due to a lack of
856 resolution of the gravimetric data.

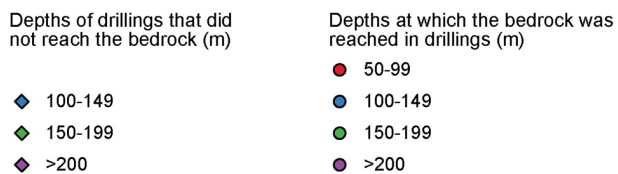
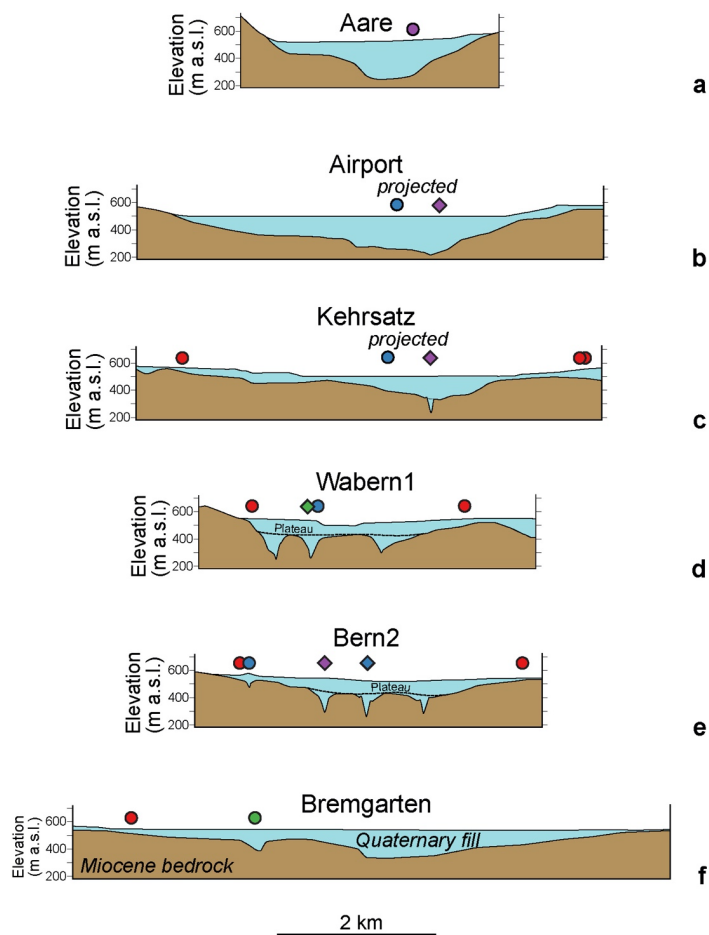


Figure 8

Figure 8: Sections through the Bern area, where the geometry of the bedrock is taken from the DEM illustrated in Figure 6. The Aare section is taken from Bandou et al. (2022). See Figures 2 and 6 for location and orientation of sections.

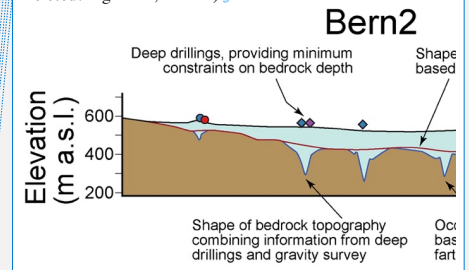
In summary, we are confronted with the situation that there is most likely a bedrock riegel imaged by the gravity data, and that thick Quaternary deposits (deep erosion) have been encountered in some deep

862 drillings as well (and have also been detected in the Bern2 gravity profile; Figures S1a to S1b in the
 863 Supplement). We thus propose an interpretation where a bedrock riegel is cut by narrow slot canyons
 864 filled with Quaternary sediments, as such a scenario adequately combines the findings from our gravity
 865 survey and drilling information. Furthermore, using the modern examples such as the Aare gorge
 866 displayed on Figure 3a as a basis, we interpret that these slot canyons formed the hydrological link
 867 between the upstream and downstream basins. We exclude an alternative interpretation where the drilled
 868 Quaternary sequences represent the filling of isolated glacial potholes. Indeed, the short distance
 869 between the individual boreholes with thick Quaternary sequences and the almost linear arrangement
 870 of these boreholes, particularly near Wabern1 (Figure 6), suggests that the drilled sequences comprise
 871 the fill of continuous channels rather than potholes.

872
 873 **5.2 Subglacial origin and the role of subglacial meltwater**

874 It is agreed upon in the literature that the formation of overdeepened basins can be understood as the
 875 response of erosion by glaciers. The main arguments that have been put forward are (i) the depths of
 876 the base of these depressions, which are generally below the current fluvial base-level, and (ii) the
 877 occurrence of adverse slopes in the downstream direction of these basins (Figure 1, Preusser et al., 2010;
 878 Patton et al., 2016; Alley et al., 2019; Magrani et al., 2022; Gegg and Preusser, 2023). Such geometric
 879 features are also encountered for the Aare main overdeepening beneath the city area of Bern. Therefore,
 880 the origin of this depression has repeatedly been interpreted as the response of the erosional processes
 881 of a glacier with a source in the Central Alps of Switzerland (Dürst Stucki et al., 2010; Preusser et al.,
 882 2010; Reber and Schlunegger, 2016; Magrani et al., 2022; Bandou et al., 2023). As a refinement already
 883 outlined by Bandou et al. (2023) and further detailed in this work, the overdeepening beneath Bern can
 884 be subdivided into a southeastern and a northwestern sub-basin. These depressions are separated by a
 885 bedrock riegel or swell, which itself is dissected by one or multiple slot canyons establishing a
 886 hydrological link between the upstream and downstream basins (Figure 6). Such ensembles of basins,
 887 riegels and slot canyons (or inner gorges) are common features in Alpine valleys (Figure 3) and have
 888 therefore been the target of previous research. In this context, it was proposed that such gorges and
 889 riegels in the Alps were likely shaped during several glacial/interglacial periods (Montgomery and
 890 Korup, 2011), and that the incision of the canyons occurred during the decay of glaciers and ice caps,
 891 when large volumes of meltwater were released (Steinemann et al., 2021). As further, yet only partly
 892 related examples, erosion by subglacial meltwater was put forward to explain the formation of inner
 893 gorges at the margin of the Fennoscandian ice sheet (based on the pattern of surface exposure ages;
 894 Jansen et al., 2014), and such a mechanism was used to explain (i) the origin of the deep channels on
 895 the floor of the eastern English Channel, and (ii) the breaching of the bedrock swell at the Dover strait
 896 during the aftermath of the Marine Isotope Stage (MIS) 12 or a later glaciation (Gupta et al., 2007;
 897 Cohen et al., 2014; Gupta et al., 2017). In this context, Jansen et al. (2014) noted that typical field
 898 evidence for inferring a subglacial meltwater control includes (i) the occurrence of anastomosing

Deleted: As summarized in Figure 1, the
 Deleted: depth
 Deleted: located
 Formatted: English (UK)
 Deleted: As outlined in the previous sections, such
 Deleted: it is not surprising that
 Formatted: English (UK)
 Deleted: Furthermore, as
 Deleted: underneath
 Deleted: additionally
 Deleted: from each other
 Deleted: Figures 1, 5 and 7).



Using geomorphic evidence in combination with information about rates
 Deleted: rock uplift and fluvial incision into bedrock, Montgomery and Korup (2011) argued that an ensemble of bedrock
 Deleted: over
 Deleted: ,
 Deleted: they were most likely formed by subglacial meltwater
 Deleted: the
 Deleted: . Such processes were particularly invoked to explain the history of inner gorge formation in the Landquart and the Trift valleys (Figures 6b, 6c) situated in the Swiss Alps (Montgomery and Korup, 2011;
 Deleted: ¶ [89]
 Deleted: occurrence
 Deleted:)
 Formatted: English (UK)
 Deleted: a

932 channels, (ii) undulating valley long profiles, and (iii) a topography that apparently amplifies the
933 hydraulic potential. The resolution of our data is not enough to see such details of the valley long
934 profiles, but sufficient to display the anastomosing patterns of the slot canyons, with channels
935 meandering, splitting and merging again (Figure 6).

937 5.3 Formation through erosion by subglacial meltwater inferred from theory and modelling
938 Besides the geometrical arguments and field-based observations outlined in the previous section, a
939 subglacial meltwater influence on the formation of overdeepenings has also been inferred based on
940 theoretical considerations, including the relationships between meltwater runoff and the sediment
941 transport capacity of proglacial and subglacial streams (e.g., Boulton and Hindmarsh, 1987; Alley et
942 al., 1997; Herman et al., 2011, Beaud et al., 2016). Because sediment transport increases exponentially
943 with both the volume and seasonality of meltwater runoff, Alley et al. (1997) interpreted that subglacial
944 and proglacial streams are among the most efficient sediment-transport mechanisms on Earth. This
945 process peaks in the ablation zone of a glacier, where surface melt reaches the bed and significantly
946 contributes to the generation of subglacial runoff. Also on theoretical grounds, Cohen et al. (2023)
947 showed that subglacial meltwater is able to remove the sediment from the base of a glacier and to further
948 incise into bedrock provided that the pressure of the subglacial meltwater and that of the ice overburden
949 are at least the same (Boulton and Hindmarsh, 1987). The results from the model of Cohen et al. (2023),
950 tailored to determine the location of the subglacial drainage pathways, further suggest that such
951 conditions most likely prevailed at the front of piedmont glaciers and particularly during the decaying
952 stage of a glacier when large volumes of meltwater were available. In addition, the model predicts that
953 under such circumstances, the locations of subglacial meltwater pathways are likely to coincide with
954 segments where high rates of glacial erosion occur (Cohen et al., 2023). Therefore, reaches with
955 evidence for intense erosion by both water and ice occur in the same area and are hydrologically
956 connected with each other, We propose this to be the case for the ensemble of overdeepened basins and
957 slot canyons beneath Bern.

959 5.4 The role of bedrock strength and the confluence of two glaciers
960 The formation of riegels and basins is consensually understood as conditioned by differences in bedrock
961 strengths. This also concerns the controls on the size of a basin itself where bedrock with a high
962 erodibility tends to host a larger basin than lithologies where the erodibility is low (e.g., Magrani et al.,
963 2020; Gegg and Preusser, 2023). Following this logic, swells preferentially would form in locations
964 where the bedrock has a lower erodibility than the rock units farther upstream and downstream. This
965 has been documented for the riegel in the Aare valley, which separates an overdeepened basin upstream
966 from a wide valley farther downstream (Figure 3a). There, the bedrock riegel is made up of the Quinten
967 Formation (Gisler et al., 2020; Stäger et al., 2020). These limestones tend to have a lower erodibility,

- Deleted: at a larger scale than...ot enough to see such (... [90])
- Deleted: 2
- Formatted (... [91])
- Formatted (... [92])
- Deleted: A...esides the geometrical arguments and fie (... [93])
- Deleted: Boultoon
- Deleted: Hindmarsch
- Formatted (... [94])
- Formatted (... [95])
- Formatted (... [96])
- Deleted: amount
- Formatted (... [97])
- Deleted: Yet, subglacial meltwater appears to play a r (... [98])
- Formatted (... [99])
- Deleted: water...eltwater is able to remove the sedin (... [100])
- Deleted: Hindmarsch (
- Formatted (... [101])
- Formatted (... [102])
- Deleted: decay
- Formatted (... [103])
- Deleted: it is not surprising that
- Formatted (... [104])
- Deleted: , as is
- Formatted (... [105])
- Deleted: Yet besides hydrological conditions, the er (... [106])
- Formatted (... [107])
- Deleted: 3
- Formatted (... [108])
- Deleted: low erosional resistance
- Deleted: erosional resistance
- Deleted: high
- Deleted: ...
- Formatted (... [109])
- Formatted (... [110])
- Formatted (... [111])
- Formatted (... [112])
- Deleted: Trift
- Deleted: (Figure 2a),
- Formatted (... [113])
- Formatted (... [114])
- Deleted: Steinemann et al., 2021).
- Deleted: forming the ridge is made up of a banded, b (... [116])
- Deleted: downstream of the confluence between the (... [118])
- Formatted (... [115])
- Formatted (... [117])
- Formatted (... [119])
- Deleted: higher mechanical strength
- Formatted (... [120])

1073 (Kühni and Piffner, 2001) than the sandstone-marl alternations (North Helvetic Flysch; Gisler et al.,
 1074 2020; Stäger et al., 2020) downstream of the bedrock swell, and the suite of sandstones, marls and
 1075 dolomite beds upstream of it (Mels- and Quarten Formations; Gisler et al., 2020; Stäger et al., 2020).
 1076 Another example is offered by the riegel in the Trift valley (Figure 3b), where the bedrock forming the
 1077 ridge is made up of a banded, biotite-rich gneiss (Erstfeld gneiss). Upstream and downstream of the
 1078 swell, the bedrock is cut by multiple faults and fractures, thus offering a lower resistance to erosion
 1079 (Steinemann et al., 2021). In the Bern area, the bedrock architecture is comparable to the examples
 1080 explained above where the UMM, which has a low erodibility, forms the swell, whereas the LFM with
 1081 a relatively large erodibility constitutes the bedrock downstream of the riegel (section 2.3). In addition,
 1082 the NW-SE striking faults in the Molasse bedrock (Isenschmid, 2019), which offer zones of mechanical
 1083 weaknesses, most likely controlled the course of the slot canyons as they have the same orientation.
 1084 Presumably as important as the contrasts in bedrock erodibility: the bedrock swell underneath Bern is
 1085 situated in the confluence area between the Valais and Aare glaciers (Figure 2b). The occurrence of
 1086 swells at the confluence areas is consistent with observations in Alpine valleys (Figure 3) and with
 1087 topographic and bathymetric DEMs of overdeepenings in Labrador, Canada (Lloyd et al., 2023). In this
 1088 case, the deep carving into the bedrock would be the result of an acceleration of the ice flow (Herman
 1089 et al., 2015) in response to the increase in the ice flux downstream of the confluence region.
 1090 Alternatively, a bedrock riegel could also form upstream of the confluence of two glaciers (see e.g., the
 1091 Maggia valley as modern example, Figure 3c). For the Bern area, the damming of the Aare glacier by
 1092 the much larger Valais glacier could have caused a reduction of the flow velocity of the Aare glacier
 1093 (Figure 2b). Consequently, the shear velocity and thus the bedrock abrasion rates would decrease,
 1094 thereby facilitating the preservation of a bedrock swell.

1095
 1096 *5.5 Differences in the geometries between the exposed riegels and basins in Alpine valleys, and the
 1097 overdeepening beneath Bern*

1098 Despite obvious similarities between the geometric properties of the overdeepening system beneath
 1099 Bern and the currently exposed riegels and slot canyons in Alpine valleys, there are also major
 1100 differences (Figure 3 versus Figures 6 and 8). The most striking one is the occurrence, beneath Bern, of
 1101 the riegel and inner gorges approximately 50-100 m below the current base-level, and the absence of
 1102 an obvious continuation of the thalweg NW of Bern (Figure 2c). Accordingly, the inferred interpretation
 1103 where the slot canyons beneath Bern were formed by subglacial meltwater requires a mechanism where
 1104 the meltwater is not only capable to incise into bedrock beneath a glacier, but also to escape the
 1105 depression by ascending nearly 200 m from the base of the overdeepening to the surface near the
 1106 glacier's snout. Using Bernoulli's principle as a basis (e.g., Batchelor, 1967), it was proposed that such
 1107 an ascent of subglacial meltwater was driven by the translation of high hydrostatic pressure into
 1108 hydrodynamic pressures at the downstream margin of a glacier (Dürst Stucki and Schlunegger, 2013).

Deleted: Piffner
 Formatted [121]
 Deleted: sandstones
 Formatted [122]
 Deleted: Stäger et al., 2020). In the Bern area, the in [123]
 Formatted [124]
 Deleted: (Garefalakis and Schlunegger, 2019). This [125]
 Formatted [126]
 Deleted: more
 Formatted [127]
 Deleted: than
 Formatted [128]
 Deleted: just upstream of
 Formatted [129]
 Deleted: 3b). As such, this situation shares many similarities
 Formatted [130]
 Deleted: the examples
 Formatted [131]
 Deleted: the
 Formatted [132]
 Deleted: where the bedrock swells are situated direct [133]
 Formatted [134]
 Deleted: 2f), directly downstream (Figures 2a, b) or [135]
 Formatted [136]
 Deleted: a trunk valley. In the same sense,
 Deleted: . (
 Deleted:) found that overdeepened basins and, as a [139]
 Formatted [137]
 Formatted [138]
 Formatted [140]
 Deleted: (Herman et al., 2015).
 Formatted [141]
 Deleted: as is the case in
 Formatted [142]
 Deleted: and Urbach valleys (
 Deleted: 2c, f). Such a situation most likely also prevailed in
 Deleted: , at least during LGM times. There
 Formatted [143]
 Formatted [144]
 Formatted [145]
 Deleted: 3b
 Formatted [146]
 Deleted: 4
 Deleted: the
 Formatted [147]
 Formatted [148]
 Deleted: , there are also major differences
 Formatted [149]
 Deleted: the
 Formatted [150]
 Deleted: 2
 Deleted: 5
 Deleted: 7
 Formatted [151]
 Formatted [152]
 Formatted [153]
 Deleted: 3c). It is indeed very unlikely that the Aare [154]
 Formatted [155]
 Deleted: large
 Deleted: pressures
 Formatted [156]
 Formatted [157]

1239 Such a mechanism is most effective at work where the surface slope of a glacier is steeper than the
 1240 adverse slope of an overdeepening (Hooke and Pohjola, 1994), as is commonly found in the frontal part
 1241 of a glacier (Figure 1a). Since the ratio between the densities of ice and water is >0.9 (Harvey, 2019),
 1242 the inferred 200 m-rise of the meltwater requires a minimum hydrostatic pressure corresponding to
 1243 >220 m-thick ice to allow an upward water flow. Such a scenario is plausible, as the Aare glacier in the
 1244 Bern area was estimated to have reached several hundred meters in thickness during past glaciations
 1245 (Bini et al., 2009; Preusser et al., 2011; Figure 2b). If this hypothesis is valid, then the thickness of the
 1246 piedmont glaciers sets an uppermost limit to the depth at which overdeepenings can be carved into the
 1247 bedrock, since it represents the driver of overpressure required for the subglacial meltwater to ascend
 1248 to the surface from deeper levels.

1250 6 Conclusions

1251 Bedrock riegels separating upstream and downstream basins are common features in modern Alpine
 1252 valleys, and they have been documented from overdeepenings in the region of Bern. We propose that
 1253 these riegels occur as ensembles together with slot canyons that cut through these swells and establish
 1254 a hydrological link between the upstream and downstream basins. We suggest this based on our
 1255 reconstruction of the bedrock topography of the Aare main overdeepening in the Bern area, and we
 1256 propose that such ensembles of basins, riegels and slot canyons also occur in other Alpine
 1257 overdeepenings such as the Rhone, Rhine and Inn valleys (Figure 9). We further suggest that these slot
 1258 canyons were formed through incision by glacial meltwater during the deglaciation when large volumes
 1259 of meltwater were available. As the flow must counteract adverse slopes, it may also be envisioned that
 1260 the slot canyons formed during glacial maxima, when ice thickness (and thus excess hydrostatic
 1261 pressure) is maximum, driving vigorous underflows. For the bedrock swell underneath Bern, the
 1262 resolution of the dataset presented in this work does not allow to locate and reconstruct the precise
 1263 course of the inferred slot canyons. However, the presented reconstruction of the bedrock topography
 1264 reconciles (i) the occurrence of low residual gravity anomalies in the Bern area (Figure 5a), which
 1265 suggests a topographic high of the incised bedrock marking the base of the overdeepening, and (ii) the
 1266 significant depth at which Quaternary sediments were encountered in drillings, indicating deep-reaching
 1267 bedrock incision (Figures 6, 7). In many Alpine valleys, such ensembles of riegel and slot canyons
 1268 appear to be preferentially formed in the confluence area between two glacial valleys and where the
 1269 bedrock has a relatively low erodibility. We posit that this configuration is also valid for the
 1270 overdeepening below the Bern area, where such a bedrock swell appears to be situated just upstream of
 1271 the confluence between the Aare and Valais glaciers, at least during LGM times and possibly during
 1272 previous glaciations. In addition, the inferred bedrock riegel beneath Bern is located where the bedrock
 1273 has a lower erodibility than farther downstream.

- Deleted: In addition, such
- Formatted ... [158]
- Deleted: 2007
- Formatted ... [159]
- Deleted: 250
- Deleted: , and it conditions the occurrence of a ... [161]
- Deleted: realistic
- Formatted ... [160]
- Formatted ... [162]
- Formatted ... [163]
- Deleted: the Aare glacier
- Deleted: m thick
- Deleted: the
- Formatted ... [164]
- Formatted ... [165]
- Formatted ... [166]
- Deleted: 3b
- Formatted ... [167]
- Deleted: mainly because sufficient pressures are req... [168]
- Moved up [4]: 1999) or MIS 11 (see discussion in Preusser
- Moved down [8]: , not only resulted in rapid glacial erosion
- Deleted: In addition, c. 6 km farther downstream fro... [169]
- Formatted ... [170]
- Deleted: are likely to be encountered in
- Deleted: . In addition, we
- Formatted ... [171]
- Formatted ... [172]
- Deleted: the
- Formatted ... [173]
- Deleted: decaying state of a glacier
- Formatted ... [174]
- Deleted: Yet
- Formatted ... [175]
- Deleted: does reconcile
- Deleted: a
- Deleted: 4a
- Formatted ... [176]
- Formatted ... [177]
- Formatted ... [178]
- Deleted: implies a relatively low bulk mass
- Deleted: Quaternary sediments
- Formatted ... [179]
- Formatted ... [180]
- Deleted: 5.
- Deleted: addition, in
- Deleted: structures
- Formatted ... [181]
- Formatted ... [182]
- Formatted ... [183]
- Deleted: hypothesis
- Formatted ... [184]
- Deleted: downstream and possibly upstream, at least... [185]
- Formatted ... [186]

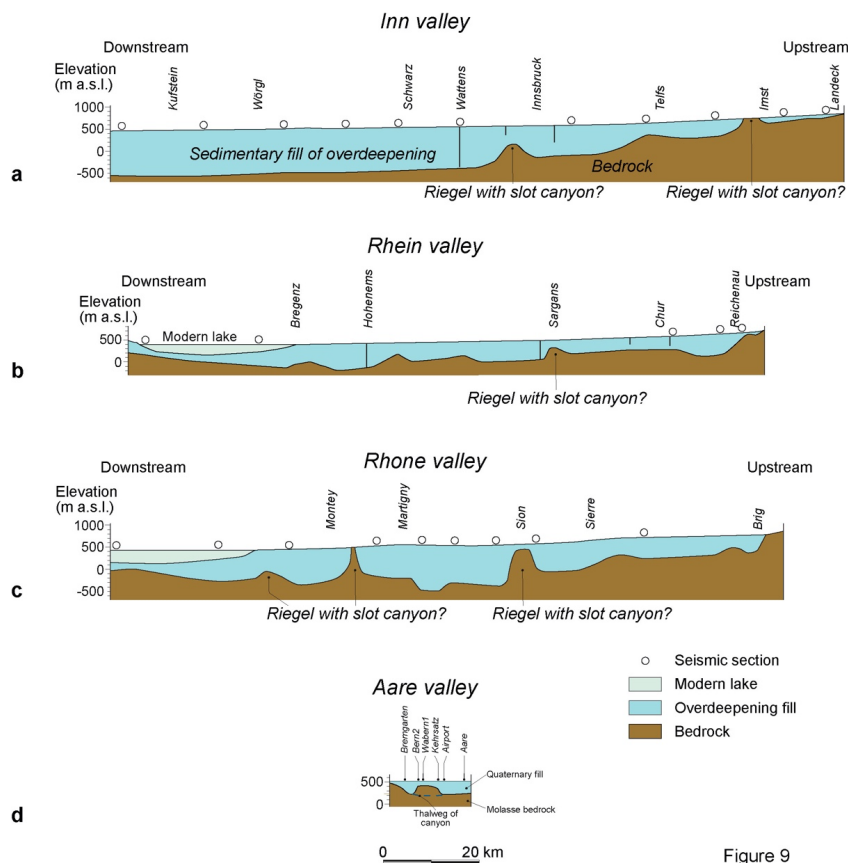


Figure 9

Figure 9: Sections showing the patterns of overdeepenings from upstream to downstream for a) the Inn valley, b) the Rhein valley, c) the Rhone valley and d) the Aare valley in the Bern area. The examples of the Inn, the Rhein and the Rhone valleys are taken from Hinderer (2001), whereas the section along the Aare valley is a modified version of Bandou et al. (2023) and bases on the data presented in Figure 6. The data from the Aare valley covers a short distance only, but it shows a striking similarity to the riegels in the large Alpine valleys. Therefore, it is quite likely that the other riegels are also dissected by narrow channels and that all settings share a similar origin.

In summary, we present a bedrock model that documents an upstream-downstream trend of the subglacial drainage network: (i) Along the Aare cross-section, which is situated upstream of the riegel there appears to be no evidence of a channelised subglacial drainage network incising into the bedrock; (ii) in the area of the inferred riegel, we postulate the occurrence of an anastomosing network of slot canyons based on drilling information, which evolves (iii) downstream of the riegel into a single canyon as seen along the Bremgarten cross-profile. This rises further questions about the mechanisms that could be responsible for these changes in the network, how such processes evolved in space and time, and how possible variations in the subglacial drainage network would have affected bedrock erosion and

1442 ice flow. Answers to such following up questions require detailed constraints on the ages and the
 1443 sedimentary architecture of the Quaternary fill, which are not available. Yet, the few chronological
 1444 information published on the Quaternary fill of overdeepenings in the Swiss Plateau does support an
 1445 interpretation where the deep carving occurred during multiple stages since the Middle Pleistocene
 1446 Transition c. 800 ka ago (Schluchter, 2004). Apparently, the change in the frequency of glacial-
 1447 interglacial cycles from a 40 ka- to a 100 ka-periodicity, which occurred at that time, not only resulted
 1448 in rapid glacial erosion (Pedersen and Egholm, 2013) and in the deep glacial carving of U-shaped
 1449 valleys in the Alps (Häuselmann et al., 2007, Valla et al., 2011), but also in the formation of
 1450 overdeepenings with complex geometries including basins, riegels and slot canyons in the foreland.

1451
 1452

1453 **Acknowledgement**

1454 This work was financially supported by the Swiss National Science Foundation (project No.
 1455 200021_175555) with contributions from the Stiftung Landschaft und Kies, swisstopo and the
 1456 Gebäudeversicherung Bern GVB.

1457 **Data availability**

1458 All data used in this paper can be ordered by the Authorities of the Canton Bern and by the authors on
 1459 request.

1460 **Author contributions**

1461 EK designed the study, together with FS and DB. DB collected the gravity data and processed them,
 1462 with support by UM and EK. FS wrote the paper and conducted the analyses and interpretation of the
 1463 data. RR drafted the bedrock topography map. PS, MS, DM and GD contributed to the discussion. All
 1464 authors approved the article.

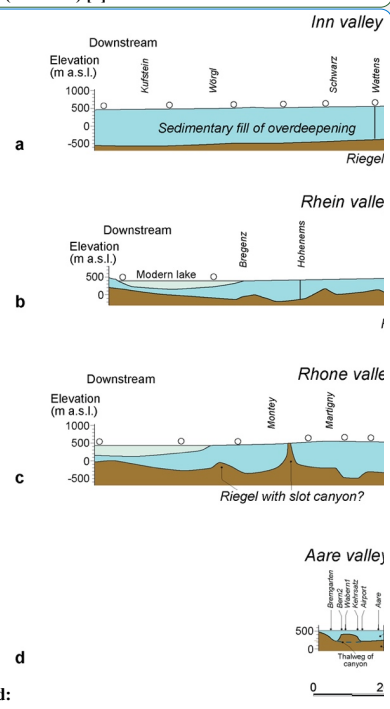
1465 **Competing interests**

1466 The authors declare that they have no conflict of interest.

1467 **References**

1468 Alley, R.B., Cuffey, K.M., Evenson, E.B., Strasser, J.C., Lawson, D.E., and Larson, G.J.: How glaciers
 1469 entrain and transport basal sediment: physical constraints. *Quat. Sci. Rev.*, 16, 1017-1038, 1997.
 1470 Alley, R., Cuffey, K., and Zoet, L.: Glacial erosion: Status and outlook. *Ann. Glaciol.*, 60, 1–13,
 1471 <https://doi.org/10.1017/aog.2019.38>, 2019.
 1472 Anderson, R.S., Molnar, P., and Kessler, M.A.: Features of glacial valley profiles simply explained. *J.*
 1473 *Geophys. Res., Earth Surface*, 111, F01004, doi:10.1029/2005JF000344, 2006.

Moved (insertion) [8]



Deleted:

- Formatted: Font: Not Bold, English (UK)
- Formatted: Centred
- Formatted: English (UK)
- Deleted: RB
- Formatted: English (UK)
- Deleted: .
- Formatted: English (UK)
- Formatted: English (UK)
- Formatted: English (UK)
- Formatted: English (UK)
- Field Code Changed

1482 Anselmetti, F., Bavec, M., Crouzet, C., Fiebig, M., Gabriel, G., Preusser, F., Ravazzi, C., and Dove
1483 team.: Drilling Overdeepened Alpine Valleys (ICDP-DOVE): quantifying the age, extent, and
1484 environmental impact of Alpine glaciations. *Sci. Drill.*, 31, 51–70. [https://doi.org/10.5194/scd-](https://doi.org/10.5194/scd-31-51-2022)
1485 31-51-2022, 2022.

1486 Bandou, D.: [Overdeepenings in the Bern region, Switzerland: Understanding their formation processes
1487 using 3D gravity forward modelling. PhD thesis, univ. Bern, Switzerland, 381pp.](https://boristheses.unibe.ch/id/eprint/4573)
1488 <https://boristheses.unibe.ch/id/eprint/4573>, 2023a.

1489 [Bandou, D.: Gravi3D: A 3D forward modelling software using gravity data to resolve the geometry of
1490 subsurface objects. https://zenodo.org/doi/10.5281/zenodo.8153258](https://zenodo.org/doi/10.5281/zenodo.8153258), 2023b.

1491 Bandou, D., Schlunegger, F., Kissling, E., Marti, U., Schwenk, M., Schläfli, P., Douillet, G., and Mair,
1492 D.: Three-dimensional gravity modelling of a Quaternary overdeepening fill in the Bern area of
1493 Switzerland discloses two stages of glacial carving. *Scientific Rep.*, 12, 1441,
1494 <https://doi.org/10.1038/s41598-022-04830-x>, 2022.

1495 Bandou, D., Schlunegger, F., Kissling, E., Marti, U., Reber, R., and Pfander J.: Overdeepenings in the
1496 Swiss plateau: U-shaped geometries underlain by inner gorges. *Swiss J. Geosci.*, 116, 19,
1497 <https://doi.org/10.1186/s00015-023-00447-y>, 2023.

1498 Banerjee, B., and [Das](#) Gupta, S.P.: Gravitational attraction of a rectangular parallelepiped. *Geophysics*,
1499 42, 1053–1055, 1977.

1500 [Batchelor](#), G. K.: An introduction to fluid dynamics (p. 615). Cambridge Univ. Press, 1967.

1501 [Beaud](#), F., [Flowers](#), G.E., and [Venditti](#), J.G.: Efficacy of bedrock erosion by subglacial water flow. *Earth
1502 Surf. Dyn.*, 4, 125-145, <https://doi.org/10.5194/esurf-4-125-2016>, 2016.

1503 [Bini](#), A., et al.: Die Schweiz während des letzteiszeitlichen Maximums (LGM) 1:500'000. Bundesamt
1504 für Landestopografie swisstopo, Bern, Switzerland, 2009.

1505 [Boulton](#), G.S., and [Hindmarsh](#), R.C.A.: Sediment deformation beneath glaciers: rheology and
1506 geological consequences. *J. Geophys. Res.* 92, 9059-9082, 1987.

1507 [Brocklehurst](#), S.H., and [Whipple](#), K.X.: Glacial erosion and relief production in the eastern Sierra
1508 Nevada, California. *Geomorphology* 42, 1–24, 2002.

1509 [Brocklehurst](#), S.H., [Whipple](#), K.X., and [Foster](#), D.: Ice thickness and topographic relief in glaciated
1510 landscapes of the western USA. *Geomorphology*, 97, 35-51,
1511 <https://doi.org/10.1016/j.geomorph.2007.02.037>, 2008.

1512 [Büchi](#), M. W., [Frank](#), S. M., [Graf](#), H. R., [Menzies](#), J., and [Anselmetti](#), F. S.: Subglacial emplacement of
1513 tills and meltwater deposits at the base of overdeepened bedrock troughs. *Sedimentology*, 64,
1514 685. <https://doi.org/10.1111/sed.12319>, 2017.

1515 [Büchi](#), M., [Graf](#), H.R., [Haldimann](#), P., [Lowick](#), S.E. and [Anselmetti](#), F.S.: Multiple Quaternary erosion
1516 and infill cycles in overdeepened basins of the northern Alpine foreland. *Swiss J. Gesci.*, 111,
1517 133-167, <https://doi.org/10.1007/s00015-017-0289-9>, 2018.

- Deleted: .
- Formatted: English (UK)
- Field Code Changed
- Formatted: English (UK)
- Formatted: English (UK)
- Formatted: English (UK)
- Formatted: English (UK)
- Field Code Changed
- Formatted: English (UK)
- Formatted: English (UK)
- Formatted: English (UK)
- Deleted: 2023
- Formatted: English (UK)
- Field Code Changed
- Formatted: English (UK)
- Formatted: English (UK)
- Formatted: English (UK)
- Formatted: English (UK)
- Formatted: English (UK)
- Field Code Changed
- Formatted: English (UK)
- Formatted: English (UK)
- Formatted: German (Switzerland)
- Formatted: German (Switzerland)
- Formatted: German (Switzerland)
- Formatted: German (Switzerland)
- Formatted: English (UK)
- Field Code Changed
- Formatted: English (UK)
- Formatted: English (UK)
- Formatted: English (UK)
- Deleted: .
- Formatted: English (UK)
- Field Code Changed
- Formatted: English (UK)
- Formatted: English (UK)
- Formatted: English (UK)
- Field Code Changed
- Formatted: English (UK)
- Formatted: English (UK)
- Formatted: English (UK)

1521 Burschil, T., Bunes, H., Tanner, D.C., Wiedlandt-Schuster, U., Ellwanger, D., and Gabriel, G.: High-
1522 resolution reflection seismics reveal the structure and the evolution of the Quaternary glacial
1523 Tannwald Basin. *Near Surf. Geophys.*, 16, 593-610, <https://doi.org/10.1002/nsg.12011>, 2018.

1524 Burschil, T., Tanner, D., Reitner, J., Bunes, H., and Gabriel, G.: Unravelling the complex stratigraphy
1525 of an overdeepened valley with high-resolution reflection seismics: The Lienz Basin (Austria),
1526 *Swiss J. Geosci.*, 112, 341–355, <https://doi.org/10.1007/s00015-019-00339-0>, 2019.

1527 Clark, P.U., and Walder, J.S. Subglacial drainage, eskers, and deforming beds beneath the Laurentide
1528 and Eurasian ice sheets. *Geol. Soc. Amer. Bull.*, 106, 304-314, [https://doi.org/10.1130/0016-7606\(1994\)106<0304:SDEADB>2.3.CO;2](https://doi.org/10.1130/0016-7606(1994)106<0304:SDEADB>2.3.CO;2), 1994.

1529
1530 Cohen, K. M., Gibbard, P. L., and Weerts, H. J. T.: North Sea palaeogeographical reconstructions for
1531 the last 1 Ma. *Neth. J. Geosci.* 93, 7–29, 2014.

1532 Cohen, D., Juvet, G., Zwinger, T., Landgraf, A., and Fischer, U.H.: Subglacial hydrology from high-
1533 resolution ice-flow simulations of the Rhine Glacier during the Last Glacial Maximum: a proxy
1534 for glacial erosion. *E&G Quat. Sci. J.*, 72, 189-201, <https://doi.org/10.5194/egqsj-72-189-201>,
1535 2023.

1536 Cook, S. J., and Swift, D. A.: Subglacial basins: Their origin and importance in glacial systems and
1537 landscapes. *Earth-Science Rev.*, 115, 332–372,
1538 <https://doi.org/10.1016/j.earscirev.2012.09.009>, 2012.

1539 Dehnert, A., Lowick, S.E., Preusser, F., Anselmetti, F.S., Drescher-Schneider, R., Graf, H.R., Heller,
1540 F., Horstmeyer, H., Kemna, H.A., Nowaczyk, N.R., Züger, and Furrer, H.: Evolution of an
1541 overdeepened trough in the northern Alpine Foreland at Niederweningen, Switzerland. *Quat.*
1542 *Sci. Rev.*, 34, 127-145, <https://doi.org/10.1016/j.quascirev.2011.12.015>, 2012.

1543 Dietrich, P., Griffis, N. P., Le Heron, D. P., Montañez, I. P., Kettler, C., Robin, C., and Guillocheau, F.:
1544 Fjord network in Namibia: A snapshot into the dynamics of the late Paleozoic glaciation.
1545 *Geology*, 49, 1521-1526, <https://doi.org/10.1130/G49067.1>, 2021.

1546 Douillet, G., Ghienne, J. F., Géraud, Y., Abueladas, A., Diraison, M., and Al-Zoubi, A.: Late Ordovician
1547 tunnel valleys in southern Jordan. *Geol. Soc. London Spec. Publ.*, 368, 275-292,
1548 <https://doi.org/10.1144/sp368.4>, 2012.

1549 Dürst Stucki, M., Reber, R., and Schlunegger, F.: Subglacial tunnel valleys in the Alpine foreland: An
1550 example from Bern, Switzerland. *Swiss J. Geosci.*, 103, 363–374,
1551 <https://doi.org/10.1007/s00015-010-0042-0>, 2010.

1552 Dürst-Stucki, M., and Schlunegger, F.: Identification of erosional mechanisms during past glaciations
1553 based on a bedrock surface model of the central European Alps. *Earth Planet. Sci. Lett.*, 384,
1554 57–70, <https://doi.org/10.1016/j.epsl.2013.10.009>, 2013.

1555 Egholm, D.L., Nielsen, S., Pedersen, V., and Lesemann, J.: Glacial effects limiting mountain height.
1556 *Nature*, 460, 884-887, <https://doi.org/10.1038/nature08264>, 2009.

Formatted [187]
Field Code Changed

Deleted: Carter, C.L., and Anderson, R.S.: Fluvial erosion of physically modeled abrasion-dominated slot canyons. *Geomorphology*, 81, 89-113, <https://doi.org/10.1016/j.geomorph.2006.04.006>, 2006.
Formatted: English (UK)
Formatted [188]
Field Code Changed

Deleted: Claude, A., Akçar, N., Ivy-Ochs, S., Schlunegger, F., Kubik, P.W., Christl, M., Vockenhuber, C., Kuhlemann, A., Rahn, M., and Schlüchter, C.: Changes in landscape evolution patterns in the northern Swiss Alpine Foreland during the mid-Pleistocene revolution. *GSA Bull.*, 131, 2056-2078, <https://doi.org/10.1130/B31880.1>, 2019.
Formatted: English (UK)
Formatted [189]
Field Code Changed

Formatted [190]
Field Code Changed

Formatted [191]
Field Code Changed

Deleted: Delaney, I., Anderson, L., and Herman, F.: Modelling the spatially distributed nature of subglacial sediment transport and erosion
Moved down [9]: . Earth Surf.
Deleted: Dyn., 11, 663-680, <https://doi.org/10.5194/esuf-11-663-2023>, 2023.
Dieleman, C., Christl, M., Vockenhuber, C., Guatschi, P., Graf, H.R., and Akçar, N.: Age of the Most Extensive Glaciation in the Alps. *Geosciences* 12, 39, <https://doi.org/10.3390/geosciences12010039>, 2022.
Formatted: English (UK)
Formatted [192]
Field Code Changed

Formatted [193]
Field Code Changed

Deleted: .
Formatted: English (UK)
Formatted [194]
Field Code Changed

Formatted [195]
Field Code Changed

Formatted [196]
Field Code Changed

1599 [Feiger, N., Huss, M., Leinss, S., Sold, L., and Farinotti, D.: The bedrock topography of Gries- and](#)
1600 [Findelengletscher. Geogr. Helv., 73, 1-9, <https://doi.org/10.5194/gh-73-1-2018>, 2018.](#)

1601 [Fischer, U., and Häberli, W.: Overdeepenings in glacial systems: Processes and uncertainties. Eos, 93,](#)
1602 [35, 341-341, <https://doi.org/10.1029/2012EO350010>, 2012.](#)

1603 [Garefalakis, P., and Schlunegger, F.: Tectonic processes, variations in sediment flux, and eustatic sea](#)
1604 [level recorded by the 20 Myr old Burdigalian transgression in the Swiss Molasse basin. Solid](#)
1605 [Earth, 10, 2045-2972, <https://doi.org/10.5194/se-10.2045-2019>, 2019.](#)

1606 Gees: Spühlbohrung Bern B1. Wasser und Energiewirtschaft des Kantons Bern, 1974.

1607 [Gegg, L., Deplazes, G., Keller, L., Madritsch, H., Spillmann, T., Anselmetti, F. S., and Büchi, M.W.:](#)
1608 [3D morphology of a glacially overdeepened trough controlled by underlying bedrock geology.](#)
1609 [Geomorphology, 394, 107950, <https://doi.org/10.1016/j.geomorph.2021.107950>, 2021.](#)

1610 [Gegg, L., and Preusser, F.: Comparison of overdeepened structures in formerly glaciated areas of the](#)
1611 [northern Alpine foreland and northern central Europa. E&G Quat. Sci. J., 72, 23-36,](#)
1612 [https://doi.org/10.5194/egqsj-72-23-2023, 2023.](#)

1613 Geotest: Grundlagen für Schutz und Bewirtschaftung der Grundwasser des Kantons Bern.
1614 Hydrogeologie Gürbetal und Stockental. Wasser- und Energiewirtschaftsamt des Kantons Bern
1615 WEA, 123 pp, 1995.

1616 [Geotest: Kernbohrung Kb 97.1. Wasser und Energiewirtschaft des Kantons Bern, 1997.](#)

1617 Gerber, E.: Geologische Karte von Bern und Umgebung 1:25'000. Kümmerli und Frei, Bern, 1927.

1618 [Gisler, C., Labhart, T., Spillmann, P., Herwegh, M., Della Valla, G., Trüssel, M., and Wiederkehr, M.:](#)
1619 [Erläuterungen. Geologischer Atlas der Schweiz 1:25'000, 1210 Innertkirchen, Schweiz. Geol.](#)
1620 [Komm., 2020.](#)

1621 [Gupta, S., Collier, J.S., Palmer-Felgate, A., and Potter, G.: Catastrophic flooding origin of shelf valley](#)
1622 [systems in the English Channel. Nature, 448, 342-345, <https://doi.org/10.1038/nature06018>,](#)
1623 [2007.](#)

1624 [Gupta, S., Collier, J. S., Garcia-Moreno, D., Oggioni, F., Trentesaux, A., Vanneste, K., De Batist, M.,](#)
1625 [Camelbeeck, T., Potter, G., Van Vliet-Lanoë, B., and Arthur, J. C. R.: Two-stage opening of](#)
1626 [the Dover Strait and the origin of island Britain. Nat. Comm., 8, 15101,](#)
1627 [https://doi.org/10.1038/ncomms15101, 2017.](#)

1628 [Häberli, W., Linsbauer, A., Cochachin, A., Salazar, C., and Fischer, U.H.: On the morphological](#)
1629 [characteristics of overdeepenings in high-mountain glacier beds. Earth Surf. Proc. Landf., 41,](#)
1630 [1980-1990, <https://doi.org/10.1002/esp.396>, 2016.](#)

1631 [Hantke, R., and Scheidegger, A. E.: Zur Genese der Aareschlucht \(Berner Oberland, Schweiz\). Geogr.](#)
1632 [Helv., 48, 120-124, <https://doi.org/10.5194/gh-48-120-1993>, 1993.](#)

1633 Harvey, A. H.: Properties of Ice and Supercooled Water, in: CRC Handbook of Chemistry and Physics
1634 (97th ed.), edited by Haynes, W. Lide, D. R. and Bruno, T., Boca Raton, FL: CRC Press., 2019.

- Formatted: English (UK)
- Field Code Changed
- Formatted: English (UK)
- Formatted: English (UK)
- Formatted: English (UK)
- Field Code Changed
- Formatted: English (UK)
- Formatted: English (UK)
- Formatted: English (UK)
- Deleted: .
- Formatted: English (UK)
- Field Code Changed
- Formatted: English (UK)
- Formatted: English (UK)
- Formatted: English (UK)
- Deleted: .
- Formatted: German (Switzerland)
- Deleted: Geyh, M.A., and Müller, H.: Palynological and geochronological study of the Holsteinian/Hoxnian/Landos interglacial, in: The Climate of Past Interglacials, edited by: Sirocko, F., Elsevier, Boston, MA, 387-396, 2007.
- Formatted: English (UK)
- Deleted: .
- Formatted: English (UK)
- Field Code Changed
- Formatted: English (UK)
- Formatted: English (UK)
- Formatted: English (UK)
- Deleted: .
- Formatted: English (UK)
- Field Code Changed
- Formatted: English (UK)
- Formatted: English (UK)
- Formatted: English (UK)
- Formatted: English (UK)
- Deleted: .
- Formatted: English (UK)
- Field Code Changed
- Formatted: English (UK)
- Formatted: English (UK)
- Formatted: English (UK)
- Deleted: 2017
- Formatted: English (UK)

1645 Häuselmann, P., Granger, D.E., Jeannin, P.-Y., and Lauritzen, S.-E.: Abrupt glacial valley incision at
1646 0.8 Ma dated from cave deposits in Switzerland. *Geology*, 35, 143-146,
1647 <https://doi.org/10.1130/G23094A>, 2007.

1648 Herman, F., and Braun, J.: Evolution of the glacial landscape of the Southern Alps of New Zealand:
1649 insights from a glacial erosion model. *J. Geophys. Res.* 113, F02009,
1650 <https://doi.org/10.1029/2007JF000807>, 2008.

1651 Herman, F., Beaud, F., Champagnac, J.-D., Lemiux, J.-M., and Sternai, P.: Glacial hydrology and
1652 erosion patterns: a mechanism for carving glacial valleys. *Earth Planet. Sci. Lett.* 310, 498–508,
1653 <https://doi.org/10.1016/j.epsl.2011.08.022>, 2011.

1654 Herman, F., Beyssac, O., Brughelli, M., Lane, S.N., Leprince, S., Adatte, T., Lin, J.Y.Y., Avouac, J.-
1655 P., and Cox, S.C.: Erosion by an Alpine glacier. *Science*, 350, 193-195,
1656 <https://doi.org/10.1126/science.aab2386>, 2015.

1657 Hinderer, M. Late Quaternary denudation of the Alps, valley and lake fillings and modern river loads.
1658 *Geodinamica Acta*, 14, 231-263, <https://doi.org/10.1080/09853111.2001.11432446>, 2001.

1659 Hooke, R.L., and Pohjola, V.A.: Hydrology of a segment of a glacier situated in an overdeepening,
1660 Storglaciären, Sweden. *J. Glaciol.*, 40, 140-148, <https://doi.org/10.3189/S0022143000003919>,
1661 1994.

1662 Isenschmid, C.: Die Grenze Untere Stüsswassermolasse/Obere Meeremolasse als Schlüssel zur Tektonik
1663 in der Region Bern. *Mitt. Natf. Ges. Bern*, 76, 108–133, 2019.

1664 Jansen, J.D., Codilean, A.T., Stroeve, A.P., Fabel, D., Hättestrand, C., Kleman, J., Harbor, J.M.,
1665 Heyman, J., Kubik, P.W., and Xu, S.: Inner gorges cut by subglacial meltwater during
1666 Fennoscandian ice sheet decay. *Nat. Comm.*, 5, 3815, <https://doi.org/10.1038/ncomms4815>,
1667 2014.

1668 Jørgensen, F., and Sandersen, P.B.E.: Buried and open tunnel valleys in Denmark—erosion beneath
1669 multiple ice sheets. *Quat. Sci. Rev.*, 25, 1339–1363,
1670 <https://doi.org/10.1016/j.quascirev.2005.11.006>, 2006.

1671 Jordan, P.: Analysis of overdeepened valleys using the digital elevation model of the bedrock surface
1672 of northern Switzerland. *Swiss J. Geosci.*, 103, 375–384, <https://doi.org/10.1007/s00015-010-0043-z>, 2010.

1673

1674 Kehew, A.E., Piotrowski, J.A., and Jørgensen, F.: Tunnel valleys: concepts and controversies – a
1675 review. *Earth-Sci. Rev.* 113, 33–58, <https://doi.org/10.1016/j.earscirev.2012.02.002>, 2012.

1676 Kellerhals, P., and Häfeli, C.: Brunnenbohrung Münsingen. *Geologische Dokumentation des Kantons*
1677 Bern, WEA-Geologie, Beilage Nr. 2, 7 pp, 1984.

1678 Kissling, E., Schwendener, H.: The Quaternary sedimentary fill of some Alpine valleys by gravity
1679 modeling. *Eclogae Geol. Helv.*, 83, 311–321, 1990.

- Field Code Changed
- Formatted: English (UK)
- Formatted: English (UK)
- Formatted: English (UK)
- Field Code Changed
- Formatted: English (UK)
- Formatted: English (UK)
- Field Code Changed
- Formatted: English (UK)
- Formatted: English (UK)
- Deleted: <https://doi.org/10.1126/science.aab2386>
- Formatted: English (UK)
- Formatted: English (UK)
- Formatted: English (UK)
- Field Code Changed
- Formatted: English (UK)
- Deleted: Ivy-Ochs, S., Kerschner, H., Reuther, A., Preusser, F., Heine, K., Maisch, M., Kubik, P. W., and Schlichter, C.: Chronology of the last glacial cycle in the European Alps. *J*
- Deleted: .., 23, 559–573. <https://doi.org/10.1002/jqs.1202>, 2008.
- Formatted: English (US)
- Formatted: English (UK)
- Formatted: English (UK)
- Formatted: English (UK)
- Formatted: English (UK)
- Field Code Changed
- Deleted: Peter B.E.
- Formatted: English (UK)
- Deleted: <https://doi.org/10.1016/j.quascirev.2005.11.006>
- Formatted: English (UK)
- Formatted: English (UK)
- Field Code Changed
- Formatted: English (UK)
- Formatted: English (UK)
- Deleted: Kamleitner, S., Ivy-Ochs, S., Manatschal, L., Akçar, N., Christl, M., Vockenhuber, C., Hajdas, I., Synal, H.-A.: Last glacial maximum glacier fluctuations (... [197])
- Formatted: English (UK)
- Deleted: Keller, B., Bläsi, H.-R.,
- Deleted: Mozley, P., and Matter, A.: Sedimentäre (... [198])
- Formatted: English (UK)
- Formatted: English (UK)

1716 Koutsodendris, A., Pross, J., Müller, U. C., Brauer, A., Fletcher, W. J., Kühl, N., Kirilova, E., Verhagen,
1717 F. T., Lücke, A., and Lotter, A. F.: A short-term climate oscillation during the Holsteinian
1718 interglacial (MIS 11c): An analogy to the 8.2ka climatic event?, *Global Planet. Chang.*, 92–93,
1719 224–235, <https://doi.org/10.1016/j.gloplacha.2012.05.011>, 2012.

1720 Krohn, C. F., Larsen, N. K., Kronborg, C., Nielsen, O. B., and Knudsen, K.: L. Litho- and
1721 chronostratigraphy of the Late Weichselian in Vendyssel, northern Denmark, with special
1722 emphasis on tunnel-valley infill in relation to a receding ice margin. *Boreas*, 38, 811–833,
1723 <https://doi.org/10.1111/j.1502-3885.2009.00104.x>, 2009.

1724 Kühni, A., and Pfiffner, O.A.: The relief of the Swiss Alps and adjacent areas and its relation to lithology
1725 and structure: topographic analysis from a 250-m DEM. *Geomorphology*, 41, 285–307,
1726 [https://doi.org/10.1016/S0169-555X\(01\)00060-5](https://doi.org/10.1016/S0169-555X(01)00060-5), 2001.

1727 Liebl, M., Robl, J., Hergarten, S., Egholm, D.L., and Stüwe, K.: Modeling large-scale landform
1728 evolution with a stream power law for glacial erosion (OpenLEM v37): benchmarking
1729 experiments against a more process-based description of ice flow (iSOSIA v3.4.3). *Geosci.
1730 Model Dev.*, 16, 1315–1343, <https://doi.org/10.5194/gmd-16-1315-2023>, 2023.

1731 Lloyd, C., Clark, C.D., and Swift, D.A.: The effect of valley confluence and bedrock geology upon the
1732 location and depth of glacial overdeepenings. *Geogr. Ann.: Series A, Phys. Geogr.*,
1733 <https://doi.org/10.1080/04353676.2023.2217047>, 2023.

1734 Lohrberg, A., Schneider von Deimling, J., Grob, H., Lenz, K.-F., and Krastel, S.: Tunnel valleys in the
1735 southeastern North Sea: More data, more complexity. *E&G Quat. Sci. J.*, 71, 267–274,
1736 <https://doi.org/10.5194/egqsj-71-267-2022>, 2022.

1737 [Magrani, F., Valla, P.G., Gribenski, N., and Serra, E.: Glacial overdeepening in the Swiss Alps and
1738 foreland: Spatial distribution and morphometrics. *Quat. Sci. Rev.*, 243, 106483,
1739 <https://doi.org/10.1016/j.quascirev.2020.106483>, 2020.](https://doi.org/10.1016/j.quascirev.2020.106483)

1740 [Magrani, F., Valla, P.G., and Egholm, D.: Modelling alpine glacier geometry and subglacial erosion
1741 patterns in response to contrasting climatic forcing. *Earth Surf. Process. Landf.*, 47, 1954–1072,
1742 <https://doi.org/10.1002/esp.5302>, 2022.](https://doi.org/10.1002/esp.5302)

1743 Moreau, J., Huuse, M., Janszen, A., van der Vegt, P., Gibbard, P. L., and Moscriello, A.: The
1744 glaciogenic unconformity of the southern North Sea. *Geol. Soc. London Spec. Publ.*, 368, 99,
1745 <https://doi.org/10.1144/SP368.5>, 2012.

1746 Montgomery, D. R., and Korup, O.: Preservation of inner gorges through repeated Alpine glaciations.
1747 *Nat. Geosci.*, 4, 62–67, <https://doi.org/10.1038/Ngeo1030>, 2011.

1748 Nagy, D.: The gravitational attraction of a right rectangular prism. *Geophysicis*, 31, 362–271, 1996.

1749 [Nishiyama, R., Ariga, A., Ariga, T., Lechmann, A., Mair, D., Pistillo, C., Scampoli, P., Valla, P.G.,
1750 Vladymyrov, M., Ereditato, A., and Schlunegger, F.: Bedrock sculpting under an active alpine](https://doi.org/10.1016/j.tecto.2019.05.011)

- Field Code Changed
- Formatted: English (UK)
- Formatted: English (UK)
- Formatted: English (UK)
- Field Code Changed
- Formatted: English (UK)
- Formatted: English (UK)
- Formatted: English (UK)
- Deleted: Lisiecki, L.E., and Raymo, M.E.: A Pliocene-Pleistocene stack of 57 globally distributed benthic d¹⁸O records. *Paleoceanography*, 20, PA1003, <https://doi.org/10.1029/2004PA001071>, 2005.
- Formatted: English (UK)
- Field Code Changed
- Formatted: English (UK)
- Formatted: English (UK)
- Formatted: English (UK)
- Field Code Changed
- Formatted: English (UK)
- Formatted: English (UK)
- Formatted: English (UK)
- Moved (insertion) [12]
- Formatted: English (US)
- Moved (insertion) [9]
- Formatted: English (UK)
- Deleted: .
- Formatted: English (UK)
- Formatted: English (UK)
- Formatted: English (UK)
- Formatted: English (UK)
- Field Code Changed
- Deleted: .
- Formatted: English (UK)
- Formatted: English (UK)
- Formatted: English (UK)
- Formatted: English (UK)
- Field Code Changed
- Formatted: English (UK)

1757 glacier revealed from cosmic-ray muon radiography. *Sci. Rep.*, 9, 6970,
1758 <https://doi.org/10.1038/s41598-019-43527-6>, 2019.

1759 [Olivier, R., Dumont, B. and Klingele, E.: Carte gravimétrique de la Suisse \(Anomalies de Bouguer\)](#)
1760 [1:500'000. Bundesamt für Landestopographie swisstopo,](#)
1761 [https://opendata.swiss/fr/dataset/schwerekarte-der-schweiz-bouguer-anomalien-1-500000,](https://opendata.swiss/fr/dataset/schwerekarte-der-schweiz-bouguer-anomalien-1-500000)
1762 [2008, 2011.](#)

1763 [Ottesen, D., Stewart, M., Brønner, M., and Batchelor, C. L.: Tunnel valleys of the central and northern](#)
1764 [North Sea \(56°N to 62°N\): Distribution and characteristics, *Mar. Geol.*, 425, 106199,](#)
1765 <https://doi.org/10.1016/j.margeo.2020.106199>, 2020.

1766 [Patton, H., Swift, D. A., Clark, C. D., Livingstone, S. J., and Cook, S. J.: Distribution and characteristics](#)
1767 [of overdeepenings beneath the Greenland and Antarctic ice sheets: Implications for](#)
1768 [overdeepening origin and evolution. *Quat. Sci. Rev.*, 148, 128–145,](#)
1769 <https://doi.org/10.1016/j.quascirev.2016.07.012>, 2016.

1770 [Pedersen, V.K., and Egholm, D.L.: Glaciations in response to climate variations preconditioned by](#)
1771 [evolving topography. *Nature*, 493, 206–201, <https://doi.org/10.1038/nature11786>, 2013.](#)

1772 [Perrouy, S., Moussirou, B., Martinod, J., Banvalot, S., Carretier, S., Gabalda, G., Monod, B., Hérail,](#)
1773 [G., Regard, V., and Remy, D.: Geometry of two glacial valleys in the northern Pyrenees](#)
1774 [estimated using gravity data, *Comptes Rendus Geosci.*, 347, 13–23,](#)
1775 <https://doi.org/10.1016/j.crte.2015.01.002>, 2015.

1776 [Piotrowski, J.A.: Subglacial hydrology in north-western Germany during the last glaciation:](#)
1777 [Groundwater flow, tunnel valleys and hydrological cycles. *Quat. Sci. Rev.*, 16, 169–185,](#)
1778 [https://doi.org/10.1016/S0277-3791\(96\)00046-7](https://doi.org/10.1016/S0277-3791(96)00046-7), 1997.

1779 [Platt, N. and Keller, B.: Distal alluvial deposits in a foreland basin setting – the Lower Freshwater](#)
1780 [Molasse \(Lower Miocene\), Switzerland: sedimentology, architecture and palaeosols,](#)
1781 [Sedimentology, 39, 545–565, <https://doi.org/10.1111/j.1365-3091.1992.tb02136.x>, 1992.](#)

1782 [Preusser, F., and Schlüchter, C. Dates from an important early Late Pleistocene ice advance in the Aare](#)
1783 [valley, Switzerland. *Eclogae Geol. Helv.*, 97, 245–253, \[https://doi.org/10.1007/s00015-004-\]\(https://doi.org/10.1007/s00015-004-1119-4\)](#)
1784 [1119-4](#), 2004.

1785 [Preusser, F., Drescher-Schneider, R., Fiebig, M., and Schlüchter, C.: Re-interpretation of the Meikirch](#)
1786 [pollen record, Swiss Alpine Foreland, and implications for Middle Pleistocene](#)
1787 [chronostratigraphy. *J. Quat. Sci.*, 20., 607–620, <https://doi.org/10.1002/jqs.930>, 2005.](#)

1788 [Preusser, F., Reitner, J. M., and Schlüchter, C.: Distribution, geometry, age and origin of overdeepened](#)
1789 [valleys and basins in the Alps and their foreland. *Swiss J. Geosci.*, 103, 407–426,](#)
1790 <https://doi.org/10.1007/s00015-010-0044-y>, 2010.

Formatted: English (UK)

Formatted: English (UK)

Formatted: English (UK)

Deleted: Nørgaard, J., Jansen, J.D., Neuhuber, S., Ruzsiczay-Rüdiger, Z., Knudsen, M.F.: P-PINI: A cosmogenic nuclide burial dating method for landscapes undergoing non-steady erosion. *Quat. Geochron.*, 74, 101420, <https://doi.org/10.1016/j.quageo.2022.101420>, 2023.

Formatted: English (UK)

Formatted: English (UK)

Formatted: English (UK)

Formatted: English (UK)

Field Code Changed

Formatted: English (UK)

Formatted: English (UK)

Formatted: English (UK)

Formatted: English (UK)

Field Code Changed

Deleted: Pfander, J., Schlunegger, F., Serra, E., Gribenski, N., Garefalakis, P., and Akçar, N.: Glaciofluvial sequences recording the Birrfeld Glaciation (MSS 5d-2) in the Bern area, Swiss Plateau. *Swiss J. Geosci.*, 115, 12, <https://doi.org/10.1186/s00015-022-00414-z>, 2022.

Formatted: English (UK)

Formatted: English (UK)

Formatted: English (UK)

Field Code Changed

Formatted: English (UK)

Moved (insertion) [11]

Formatted: English (UK)

Deleted: .

Formatted: English (UK)

Formatted: English (UK)

Field Code Changed

Formatted: English (UK)

Formatted: English (UK)

Formatted: English (UK)

Formatted: English (UK)

Formatted: English (UK)

Field Code Changed

Deleted: .

Formatted: English (UK)

Formatted: English (UK)

Formatted: English (UK)

Formatted: English (UK)

Field Code Changed

1804 Preusser, F., Graf, H. R., Keller, O., Krayss, E., and Schlüchter, C.: Quaternary glaciation history of
1805 Northern Switzerland. *E&G Quat. Sci. J.*, 60, 282–305, <https://doi.org/10.3285/eg.60.2-3.06>,
1806 2011.

1807 Reber, R., and Schlunegger, F.: Unravelling the moisture sources of the Alpine glaciers using tunnel
1808 valleys as constraints. *Terra Nova*, 28, 202–211, <https://doi.org/10.1111/ter.12211>, 2016.

1809 Reitner, J.M., Gruber, W., Römer, A., and Morawetz, R.: Alpine overdeepenings and paleo-ice flow
1810 changes: an integrated geophysical-sedimentological case study from Tyrol (Austria). *Swiss J.*
1811 *Geosci.*, 103, 385–405, <https://doi.org/10.1007/s00015-010-0046-9>, 2010.

1812 Roger, S., Féraud, G., de Beaulieu, J.-L., Thouveny, N., Coulon, Ch., Choucem., J.J., Andrieu, V. and
1813 Williams, T.: 40Ar/39Ar dating on tephra of the Velay maars (France): implications for the
1814 Late Pleistocene proxy-climatic record. *Earth Planet Sci. Lett.*, 170: 287–299, 1999.

1815 Ross, N., Siegert, M.J., Woodward, J., Smith, A.M., Corr, H.F.J., Bentley, M.J., Hindmarsh, R.C.A.,
1816 King, E.C., and Rivera, A.: Holocene stability of the Amundsen-Weddell ice divide, West
1817 Antarctica. *Geology*, 39, 935–938, <https://doi.org/10.1130/G31920>, 2011.

1818 Rosselli, A., and Raymond, O. : Modélisation gravimétrique 2.5D et cartes des isohypses au 1:100'000
1819 du substratum rocheux de la Vallée du Rhône entre Villeneuve et Brig (Suisse). *Eclogae Geol.*
1820 *Helv.*, 96, 399–423, 2003.

1821 Schaller, S., Büchi, M.W., Schuster, B., and Anselmetti, F.: Drilling into a deep buried valley (ICDP
1822 DOVE): a 252 m long sediment succession from a glacial overdeepening in northwestern
1823 Switzerland. *Sci. Drill.*, 32, 27–42, <https://doi.org/10.5194/sd-32-27-2023>, 2023.

1824 Schläfli, P., Gobet, E., van Leeuwen, J.F.N., Vescovi, E., Schwenk, M.A., Bandou, D., Douillet, G.A.,
1825 Schlunegger, F., and Tinner, W.: Palynological investigations reveal Eemian interglacial
1826 vegetation dynamics at Spiezberg, Bernese Alps, Switzerland. *Quat. Sci. Rev.*, 263, 106975,
1827 <https://doi.org/10.1016/j.quascirev.2021.106975>, 2021.

1828 Schlüchter, C.: Thalgut: ein umfassendes [eiszeitstratigraphisches](https://doi.org/10.1016/S1571-0866(04)80092-7) Referenzprofil im nördlichen
1829 Alpenvorland. *Eclogae geol. Helv.*, 82, 277–284, 1989.

1830 Schlüchter, C. The Swiss glacial record – a schematic summary. *Develop. Quat. Sci.*, 2, 413–418,
1831 [https://doi.org/10.1016/S1571-0866\(04\)80092-7](https://doi.org/10.1016/S1571-0866(04)80092-7), 2004.

1832 Schlunegger, F., and Garefalakis, P.: Einführung in die Sedimentologie, Schweizerbart, Stuttgart,
1833 www.schweizerbart.de/9783510655397, 2023.

1834 Schwenk, M., Schläfli, P., Bandou, D., Gribenski, N., Douillet, G., and Schlunegger, F.: From glacial
1835 erosion to basin overfill: A 240 m-thick overdeepening-fill sequence in Bern. Switzerland. *Sci.*
1836 *Drill.*, 30, 17–42, <https://doi.org/10.5194/sd-30-17-2022>, 2022a.

1837 Schwenk, M. A., Stutenbecker, L., Schläfli, P., Bandou, D., and Schlunegger, F.: Two glaciers and one
1838 sedimentary sink: The competing role of the Aare and the Valais glaciers in filling an

Formatted: English (UK)

Formatted: English (UK)

Formatted: English (UK)

Field Code Changed

Moved up [12]: . Rev.,

Deleted: Preusser, F., Büschelberger, M., Kemma, H.A., MIOCIC, J., Müller, D. and May, J.-H.: Exploring possible links between Quaternary aggradation in the Upper Rhine Graben and the glaciation history of northern Switzerland. *Int. J. Earth Sci.*, 110, 1827–1846, <https://doi.org/10.1007/s00531-021-02043-7>, 2021. [↗](#)
Raisback, L.B., Gibbard, P.L., Head, M.J., Voarintsoa, N.R.G., and Toucanne, S.: An optimized scheme of lettered marine isotope substages for the last 1.0 million years, and the climatostratigraphic nature of isotope stages and substages. *Quat. Sci*

Deleted: 111, 94–106, 10.1016/j.quascirev.2015.01.012, 2015. [↗](#)

Reber, R., Akçar, N., Ivy-Ochs, S., Tikhomirov, D., Burkhalter, R., Zahno, C., Lüthold, A., Kubik, P.W., Voekenhuber, C., and Schlüchter, C.: Timing of retreat of the Reuss Glacier (Switzerland) at the end of the Last Glacial Maximum. *Swiss J. Geosci.*, 107, 293–307, <https://doi.org/10.1007/s00015-014-0169-5>, 2014. [↗](#)

Formatted: English (UK)

Formatted: English (UK)

Formatted: English (UK)

Formatted: English (UK)

Field Code Changed

Formatted: English (UK)

Field Code Changed

Formatted: English (UK)

Formatted: English (UK)

Deleted: Schlüchter, C.: The deglaciation of the Swiss-Alps: a paleoclimatic event with chronological problems. *Bull. l'Association française pour l'étude du Quat.*, 25, 141–145, 1988. [↗](#)

Deleted: eiszeit stratigraphisches

Formatted: English (UK)

Formatted: English (UK)

Formatted: English (UK)

Formatted: English (UK)

Field Code Changed

Formatted: English (UK)

Formatted: English (UK)

Formatted: English (UK)

Formatted: English (UK)

Field Code Changed

1864 overdeepened trough inferred from provenance analysis. *E&G Quat. Sci. J.*, 71, 163–190,
1865 <https://doi.org/10.5194/egqsj-71-163-2022>, 2022b.

1866 [Stäger, D., Labhart, T., Della Valle, G., Tröhler, B., Schwarz, H., Gisler, C., Rathmayr, B. and](#)
1867 [Wiederkehr, M. Blatt 1210 Innertkirchen. Geol. Atlas Schweiz 1:25'000, Karte 167, Swisstopo,](#)
1868 [2020.](#)

1869 [Steinemann, O., Ivy-Ochs, S., Hippe, K., Christl, M., Naghipour, N., and Synal, H.-A.:](#) Glacial erosion
1870 by the Trift glacier (Switzerland): Deciphering the development of riegels, rock basins and
1871 gorges. *Geomorphology*, 375, 107533, <https://doi.org/10.1016/j.geomorph.2020.107533>, 2021.

1872 Stewart, M.A., and Lonergan, L.: Seven glacial cycles in the middle-late Pleistocene of northwest
1873 Europe: geomorphic evidence from buried tunnel valleys. *Geology* 39, 283-286,
1874 <https://doi.org/10.1130/G31631.1>, 2011.

1875 Stewart, M.A., Lonergan, L. and Hampson, G.: 3D seismic analysis of buried tunnel valleys in the
1876 central North Sea: tunnel valley-fill sedimentary architecture, in: *Glaciogenic Reservoirs and*
1877 *Hydrocarbon Systems*, edited by: Huuse, M., Redfern, J., Le Heron, D.P., Dixon, R.J., and
1878 Moscardiello, A.. *Geol. Soc. London Spec. Publ.*, 368, 173-183,
1879 <http://dx.doi.org/10.1144/SP368.9>, 2013.

1880 Valla, P.G., van der Beek, P.A., and Carcaillet, J.: Dating bedrock gorge incision in the French Western
1881 Alps (Ecrins-Pelvoux massif) using cosmogenic ¹⁰Be. *Terra Nova*, 22, 18-25,
1882 <https://doi.org/10.1111/j.1365-3121.2009.00911.x>, 2010.

1883 Valla, P., Shuster, D.L., and van der Beek, P.A.: Significant increase in relief of the European Alps
1884 during mid-Pleistocene glaciations. *Nat. Geosci.*, 4, 688-692,
1885 <https://doi.org/10.1038/ngeo1242>, 2011.

1886 Welten, M.: Pollenanalytische Untersuchungen im jüngeren Quartär des nördlichen Alpenvorlandes der
1887 Schweiz. *Beitr. Geol. Karte Schweiz*, 156, 174 pp., 1982.

1888 Welten, M.: Neue pollenanalytische Ergebnisse über das jüngere Quartär des nördlichen
1889 Alpenvorlandes der Schweiz (Mittel-und Jungpleistozän). *Beitr. Geol. Karte Schweiz*, 162, 9-
1890 40, 1988.

1891 Wright, H. E.: Tunnel valleys, glacial surges, and subglacial hydrology of the Superior Lobe, 340
1892 Minnesota. *Mem. Geol. Soc. Amer.*, 136, 251-276, <https://doi.org/10.1130/MEM136-p251>,
1893 1973.

1894 Zwahlen, P., Tinner, W. and Vescovi, E.: Ein neues EEM-zeitliches Umweltarchiv am Spiezberg
1895 (Schweizer Alpen) im Kontext der mittel- und spätpleistozänen Landschaftsentwicklung. *Mitt.*
1896 *Naturf. Ges. Bern* 78, 92–121, 2021.

Formatted: English (UK)

Formatted: English (UK)

Formatted: English (UK)

Formatted: English (UK)

Field Code Changed

Formatted: English (UK)

Formatted: English (UK)

Formatted: English (UK)

Field Code Changed

Deleted: 1321

Formatted: English (UK)

Formatted: English (UK)

Formatted: English (UK)